REPORT ON GEOLOGICAL SURVEY OF CENTRAL SULAWESI, INDONESIA

Vol. III

AEROMAGNETIC SURVEY

March 1971

OVERSEAS TECHNICAL COOPERATION AGENCY

GOVERNMENT OF JAPAN

ABSTRACT

An airborne magnetic and photographic survey of the west-central part of the Island of Sulawesi, Indonesia, has been completed. This regional survey was done for purposes of mineral exploration: to extend geological mapping of structural and lithological units on the basis of changes in rock magnetization.

This report describes the operations connected with the airborne survey, instrumentation and data recording, associated ground geophysical investigations, data reduction and compilation, and data analysis and interpretation.

The following is a summary of the principal results of the aeromagnetic interpretation;

1. General Nature of Data

   From energy spectrum analysis two magnetic components could be identified in the aeromagnetic data;

   (a) near-surface effects originated from within a few hundred meters of ground level and including topographic effects;

   (b) substantial regional anomalies which in part reflect regional changes in rock magnetization as well as magnetized sources at great depth.

2. Lithology

Granitic rocks occupying a major part of the survey area were found to have little or no magnetic expression. Based on magnetic susceptibility determinations these rocks have a very low magnetite content; less than 0.1%.

Sediments, slate and crystalline schist units were also generally found to be virtually non-magnetic.

Gneissic zones were found to be appreciably magnetic and generally could be identified as distinct from surrounding granitic rock.

Areas of basic and ultrabasic igneous intrusion and extrusion including gabbro and andesites were generally associated with large amplitude anomalies reflecting magnetite content in the order of 0.5 to 2%. Eleven distinct zones of basic intrusion were interpreted. The appropriate size and the intense magnetization of these zones suggest that some of them may have been cores of ancient volcanoes.

Volcanic members within sedimentary sections of the Mamudju-Doda Embayment adjacent to the Strait of Makassar and in the Tawaëlia Graben in the southeast part of the area, were evident by moderate to large amplitude anomaly patterns and changes in their associated magnetic expression served to delineate normal faults which appeared to play a large part in the development of both depressions.

3. Structure

The Palu Fault zone is seen in the magnetics as a virtually continuous lineament extending across the survey area. Areas west and east of this major structure appear to be structurally and to some extent lithologically distinct.

The western limit of an extensive metamorphic zone occupying the eastern margins of the survey area appears to be marked by faulting. The Tawaelia Graben is part of this fault system and is filled by a sequence of sedimentary rocks which appear to include highly magnetic volcanic members. This fault pattern appears to have been dislocated by a system of long NE-SW and westerly-trending faults that can be traced over long distances. Northerly, NE-SW and NW-SE trending faults which are probably associated with the development of the sedimentary basin adjacent to the Strait of Makassar can be identified from magnetic anomalies which are probably due to intrasedimentary volcanics.

CONTENTS

List of Figures

List of Tables

List of Attached Maps

1. INTRODUCTION

In September 1970, the Overseas Technical Cooperation Agency (OTCA) authorized the commencement of the aerial survey phases of a general mineral exploration programme covering Indonesian Department of Mines Block 4 located in the west-central part of the Island of Sulawesi.

The general requirement of the airborne geophysical survey phase reported here, was to execute and interpret an aeromagnetic reconnaissance. It was also required that the airborne geophysical work be integrated, operationally and technically, with a concurrent photogeological study.

Under Permits issued by the Indonesian Authorities in late September, flight operations began from a base at Palu, Sulawesi, on September 28, 1970.

1-1 AREA DESCRIPTION

As shown in the map, Figure 1, Sulawesi Block 4 is located in the west-central part of the Island of Sulawesi, Indonesia, lying between Latitudes 1° South and 2° South, and between the Strait of Makassar and 120°28'27.79" East Longitude.

The land area of Block 4 is approximately 14,300 square kilometers, and is characterized largely by mountainous, forest-covered terrain eastwards from sea-level to almost 3,000 meters altitude. The shade-relief map, Figure 2, shows a small coastal plain along the Makassar Strait at the west, and emphasizes the Palu River valley which dissects the mountainous central area in a NNW-SSE direction.

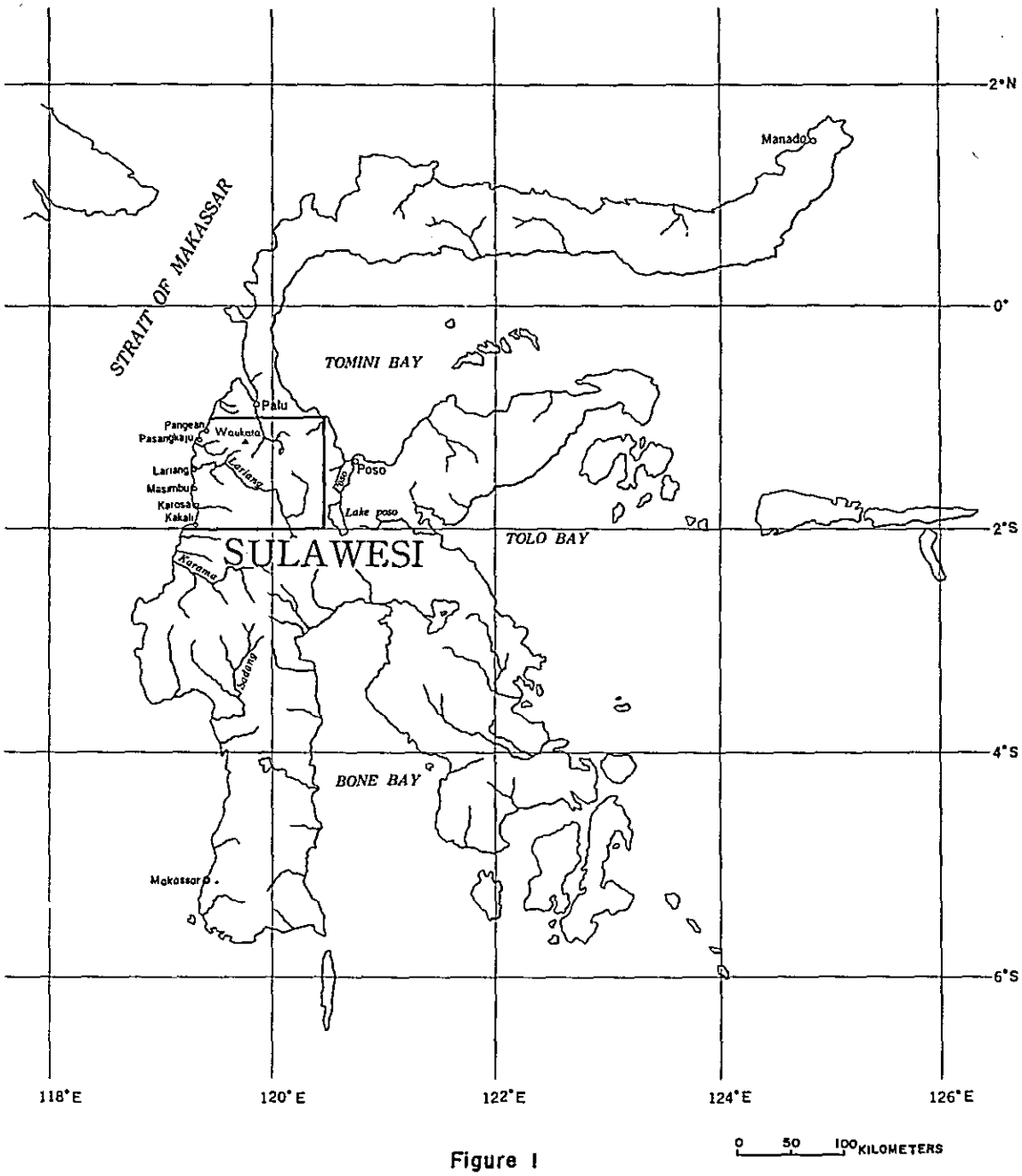

Figure 1

LOCATION MAP

WEST-CENTRAL SULAWESI AREA

AEROMAGNETIC SURVEY

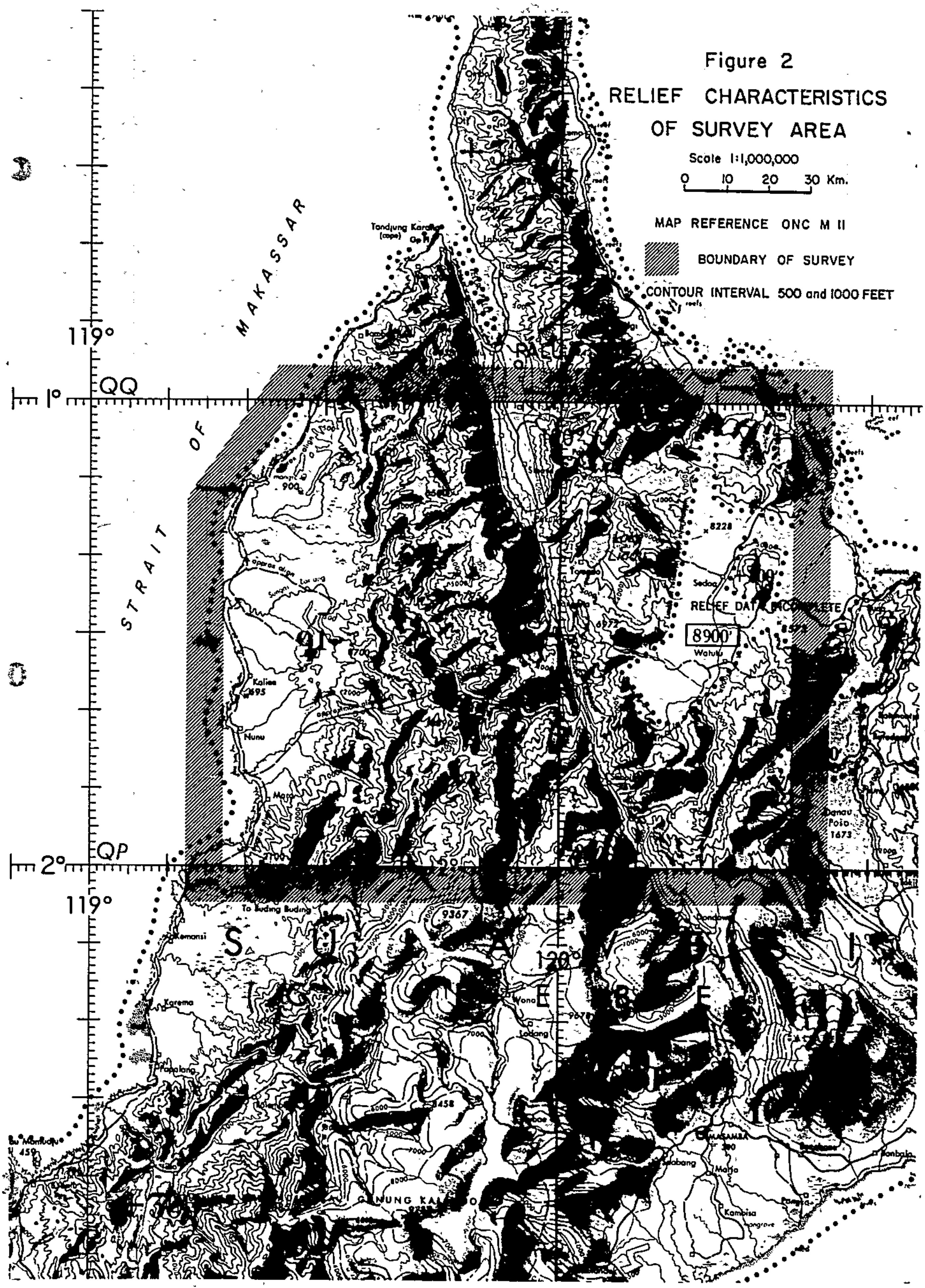

Figure 2
RELIEF CHARACTERISTICS OF SURVEY AREA

Ground access from exterior points is very limited. The airfield at Palu is connected by irregular flights with the Regional Capital at Makassar, Sulawesi; and access by sea is by means of a small port at Donggala.

The annual rainfall maxima occur in April and November, with a distinct minimum rainfall period centred on August. The aerial survey was carried out near the end of the optimum flying period, during gradually deteriorating weather.

1-2 INTEGRATION OF THE GENERAL EXPLORATION PROGRAMME

During project planning, a phase relations chart was prepared as a reference for the various participants in the aerial and ground work. A generalization of this flow chart, Figure 3, indicates the large degree of inter-dependence of the aerial photographic, geophysical, ground geological and photogeological aspects of the work. In general, the original plan has been adhered to, with minor adjustments to accommodate problems of timing especially.

Figure 3

GENERALIZED FLOW-CHART

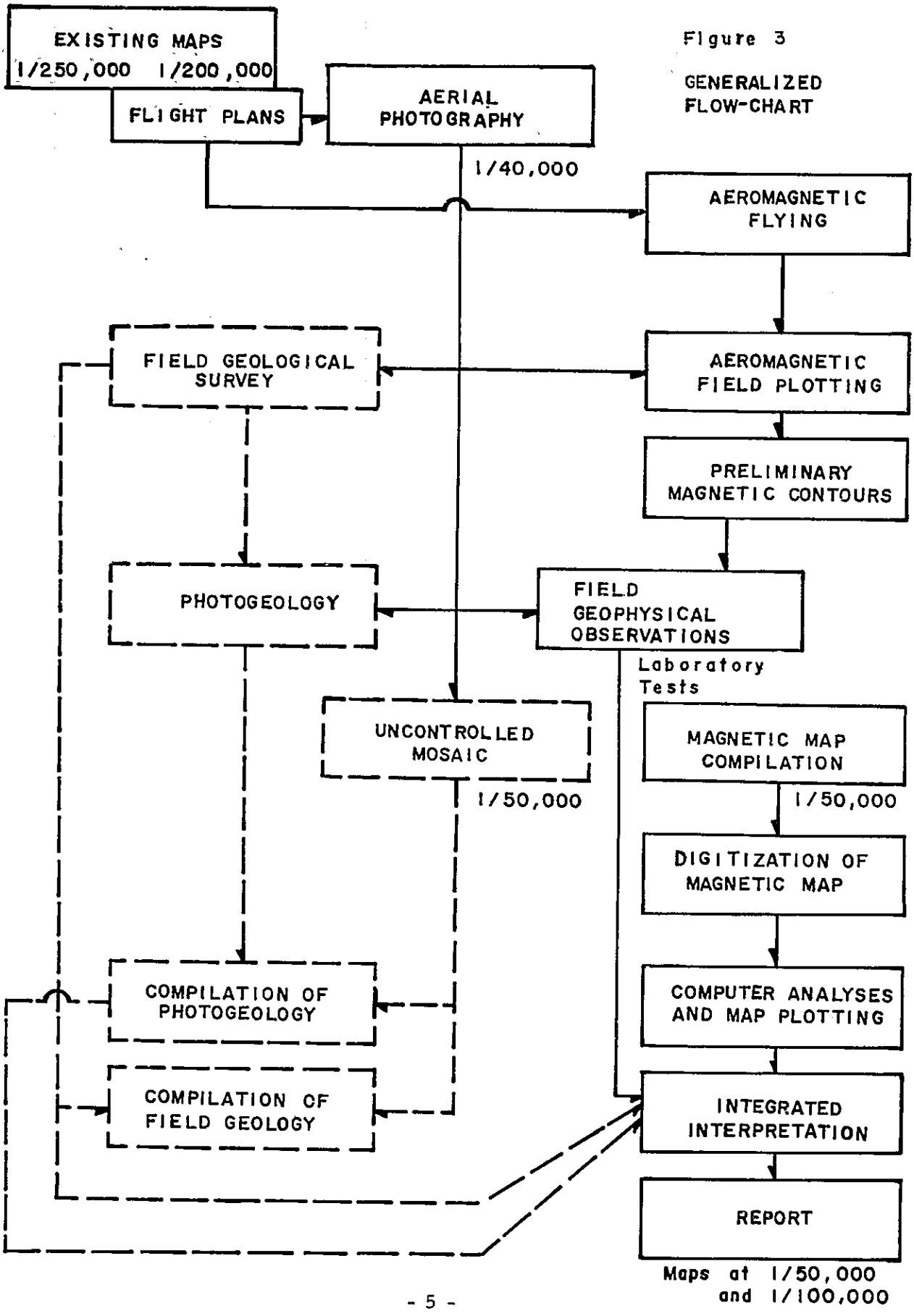

2. SURVEY OPERATIONS

The survey area was partly covered many years ago by trimetrogon photographic strips used to prepare provisional 1/250,000 scale, 100 meter contour topographic maps (see AME Series T503, Sheet SA-50.8 Pasangkaju). A separate series of Indonesian Government 1/200,000 scale planimetric maps covers the survey area; this series is considered to be a re-compilation from various sources. For purposes of survey flight navigation, these two published maps were redrawn into a special topographic map at 1/100,000 scale, incorporating the more reliable features of both.

2-1 CONCEPT OF COMBINED AEROMAGNETIC AND PHOTOGRAPHIC SURVEY OPERATIONS

The general OTCA exploration programme called for aerial photography, to be used for geological interpretation and mapping. It was anticipated that aerial photography can be performed on only about one day in six, during the dry season of Indonesia. It was therefore practical to assign a combined aeromagnetic and photographic survey aircraft to permit aeromagnetic surveying to be done on days when cloud cover precluded photography.

Doppler navigation permits reconnaissance aeromagnetic surveying to be done with acceptable accuracy, using a topographic map such as that prepared at 1/100,000, for general positioning, in advance of the preparation of a photomosaic.

2-2 AEROMAGNETIC AND PHOTOGRAPHIC FLIGHT PATTERNS

Specifications for aeromagnetic surveying called for flights in a north-south direction, at 1.5 km. spacing, and at a mean height of 250 m. above terrain. The topographic features of survey area, however, are largely rugged as described previously. It was therefore chosen to operate at a mean height of 600 m. above terrain for extra safety of the aircraft. The north-south direction is optimum for accurate magnetic field mapping in equatorial regions. The flight height 600 m. is comparable to that recommended by Malahoff (1969) for optimal aeromagnetic surveying over areas of high relief such as volcanoes; 500 m. above highest terrain.

For the small sedimentary basin along the Strait of Makassar a flight spacing of 4.5 km. was used.

Crossing E-W control profiles were flown at intervals of 7.5 minutes of Latitude; about 14 km. apart.

Specifications for aerial photography called for flights in a north-south direction, at a mean scale of 1/40,000. Using a super-wide-angle cartographic camera with 88 mm. lens, the required flight height is 4,000 m. above mean ground elevation along each flight strip. Due to the extreme variations of terrain elevation, flying heights ranging gradually from 4,000 m. above sea-level (ASL) at the coast to 5,300 m. ASL inland, were used, at a spacing of 6.2 kilometers. E-W tie-lines were flown at each 30 minutes of Latitude, being 55 kilometers apart, with an additional tie-line along the Palu River valley.

Use of the super-wide-angle camera permits 1/40,000 scale photography with a geophysical type aircraft. Equally important, the relatively low flight altitude that is sufficient in using this camera allowed flying below high cloud, and produced photography less affected in quality by atmospheric haze.

2-3 AIRCRAFT INSTRUMENTATION AND DATA RECORDINGS

The aircraft assigned was a twin-engined Aero Commander, Type 680E, equipped with long-range tanks.

The sensor of a Gulf Mark III fluxgate magnetometer was installed in the tail 'stinger' of the Aero Commander. Ancillary equipment consisted of the following:

Radio Altimeter	: Honeywell HG9050
Doppler Navigation System	: Marconi Type 623
Drift Meter	: B-3 gyro-stablized
Tracking Camera	: 35 mm. C.A.R.L. Mark VII discrete frame

On days suitable for photography, a Wild RC-9 camera (88 mm. super-wide-angle lens, 228 x 228 mm. negative format) was substituted for the Gulf Magnetometer console and 35 mm. tracking camera, for purposes of high altitude aerial photography. The RC-9 camera used the same aircraft opening (in the aircraft mid-section) as that used for the 35 mm. camera.

This equipment and associated data recordings are described as follows:

2-3-1 Gulf Mk.III Airborne Magnetometer

This is a saturable-core fluxgate magnetometer which is sensitive to magnetic field variations of about 1/2 gamma.

The magnetometer head consists of two saturable core orienting fluxgates whose axes are at right angles to one another. The axis of the measuring fluxgate is normal to the plane containing the two orienting fluxgates. In operation, self-orienting fluxgates are maintained by servomotors in a position of minimum coupling with the earth's magnetic field; the measuring fluxgate is then in a position of maximum coupling with the earth's field.

Output from the airborne magnetometer was recorded in analogue form in red ink on a moving chart paper. Sample copies of the airborne magnetometer data recordings are shown in Figures 4a and 4b. Operating range was selected as 300 gammas across a chart width of 25.4 cm.. Chart speed was such that 1 cm. is approximately equal to 0.5 km.. Records over areas of typically low and high magnetic relief are shown in Figures 4a and 4b.

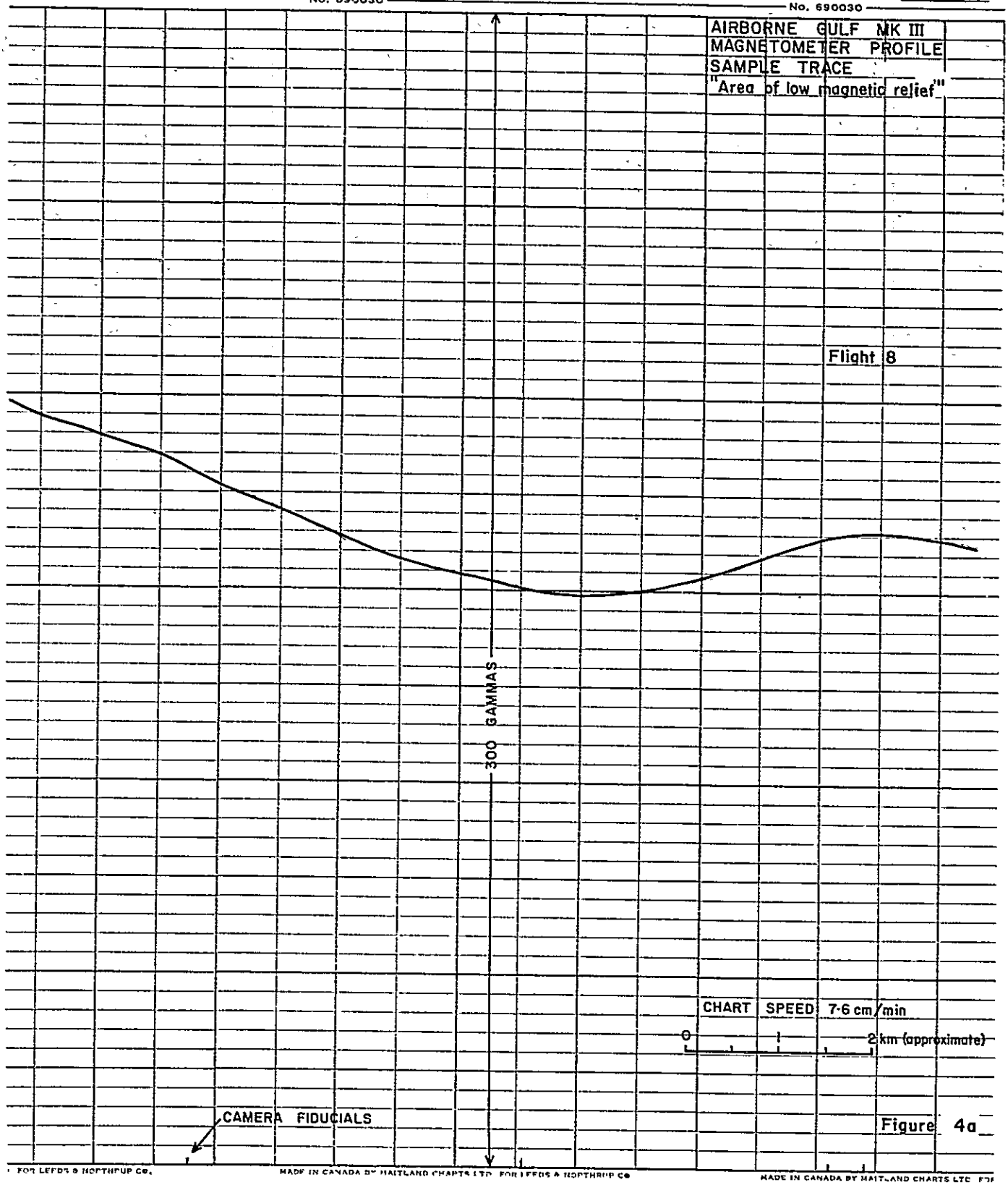
No. 690030
No. 690030
AIRBORNE GULF MK III
MAGNETOMETER PROFILE
SAMPLE TRACE
"Area of low magnetic relief"
Flight 8
300 GAMMAS
CHART SPEED 7·6 cm/min
0
2 km (approximate)
CAMERA FIDUCIALS
MADE IN CANADA BY HAITLAND CHARTS LTD. FOR LEEDS & NORTHRUP CO.

Figure 4a

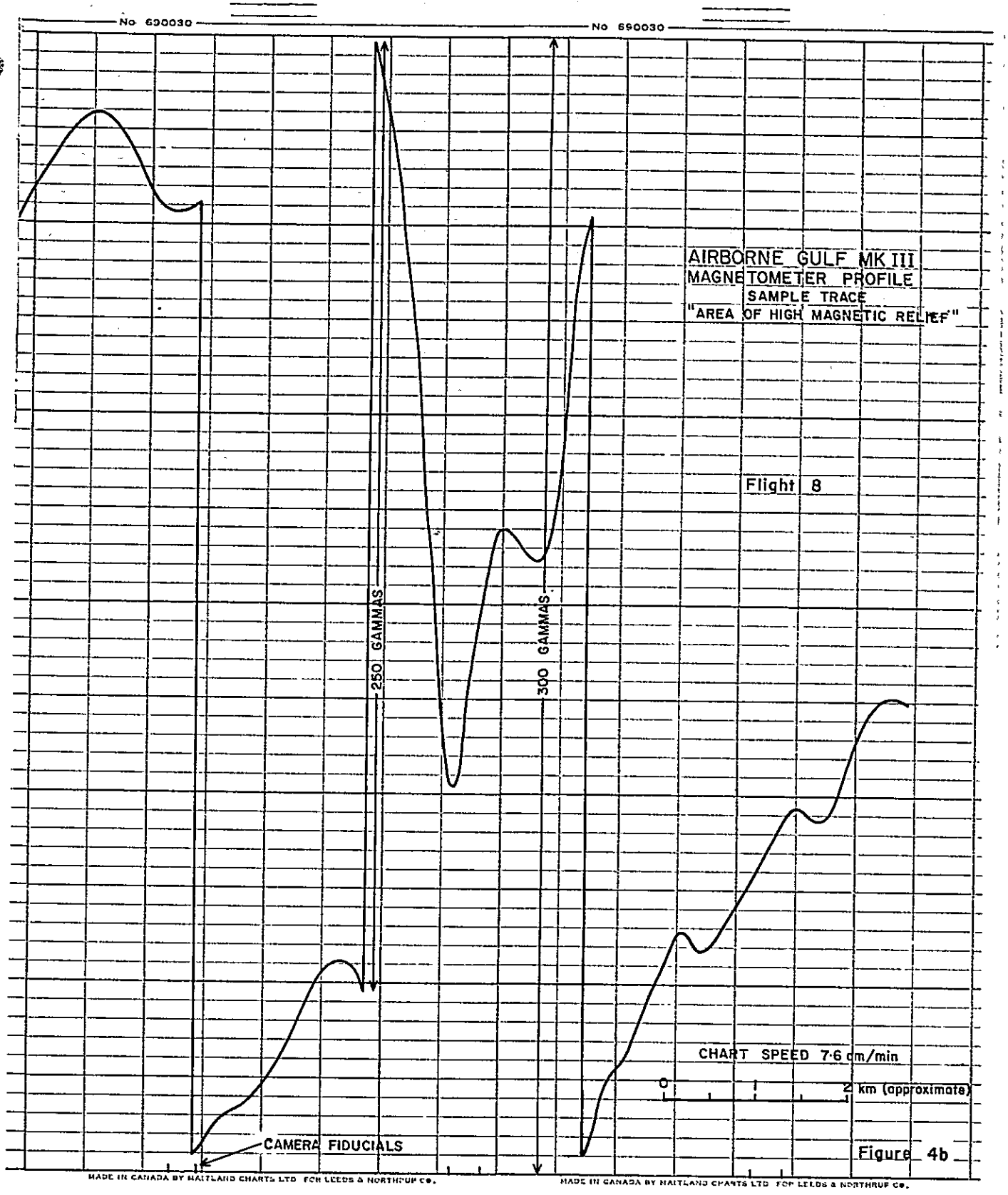
No 690030
No 690030
AIRBORNE GULF MK III
MAGNETOMETER PROFILE
SAMPLE TRACE
"AREA OF HIGH MAGNETIC RELIEF"
Flight 8
250 GAMMAS
300 GAMMAS
CHART SPEED 7·6 cm/min
0
2 km (approximate)
CAMERA FIDUCIALS
MADE IN CANADA BY MAITLAND CHARTS LTD FOR LEEDS & NORTHRUP Co.
MADE IN CANADA BY MAITLAND CHARTS LTD FOR LEEDS & NORTHRUP Co.

Figure 4b

2-3-2 Gulf Mk.I Storm Monitor

This instrument is designed to record time dependent variations in the earth's total magnetic field such as caused by magnetic storms. During periods of these disturbances, surveying is discontinued.

The instrument consists of a manually oriented saturable core fluxgate magnetometer detector mounted on a tripod with remote console and recorder.

Output from the monitor was recorded in continuous graph form on a curvilinear chart having a width of 11.4 cm.. Chart speed was 30.5 cm. per hour. Figure 5 shows a sample of a monitor magnetometer recording.

Full scale deflection represents a change in magnetic intensity of 250 gammas.

Hourly reference marks were recorded by a fiducial pen on the side of the recording chart.

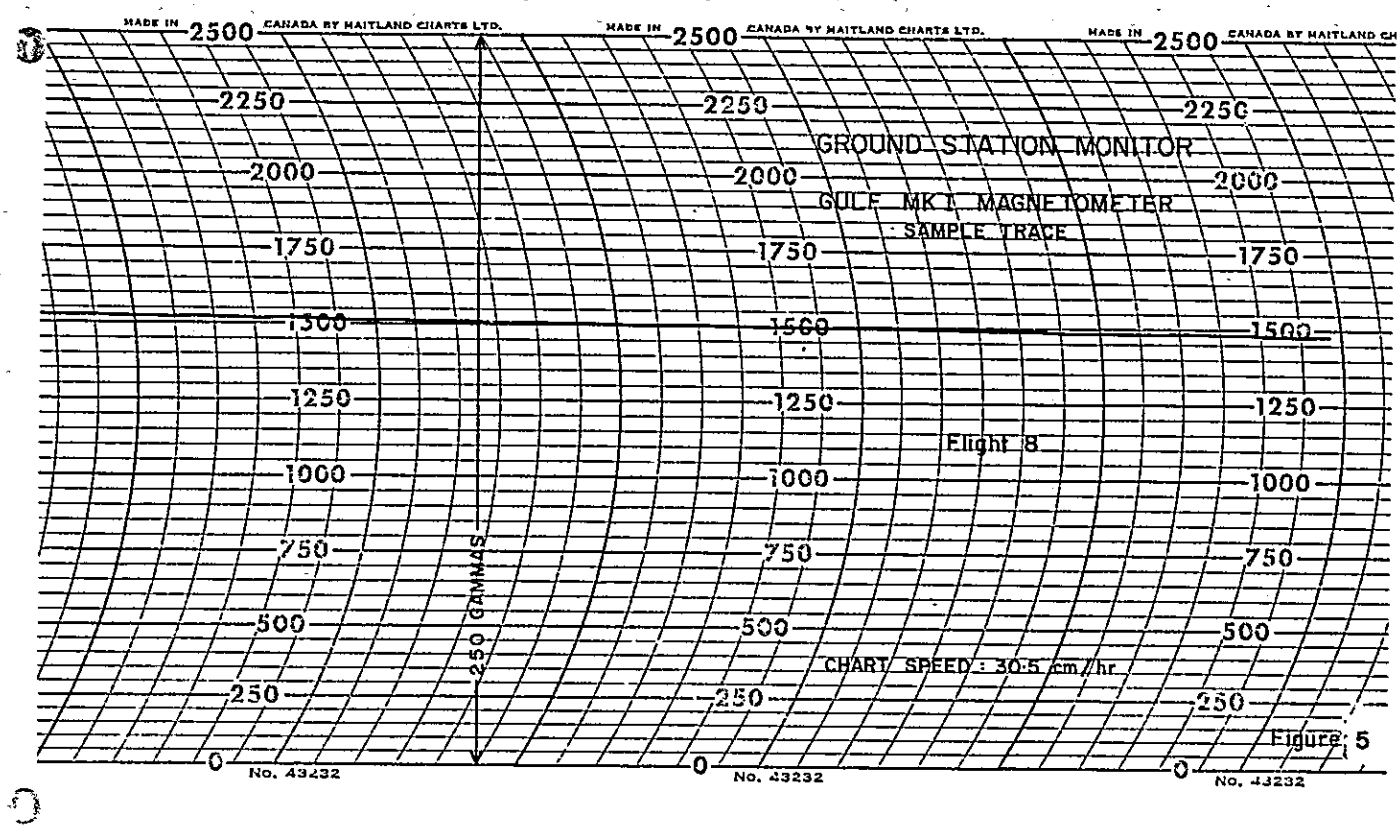

Figure 5

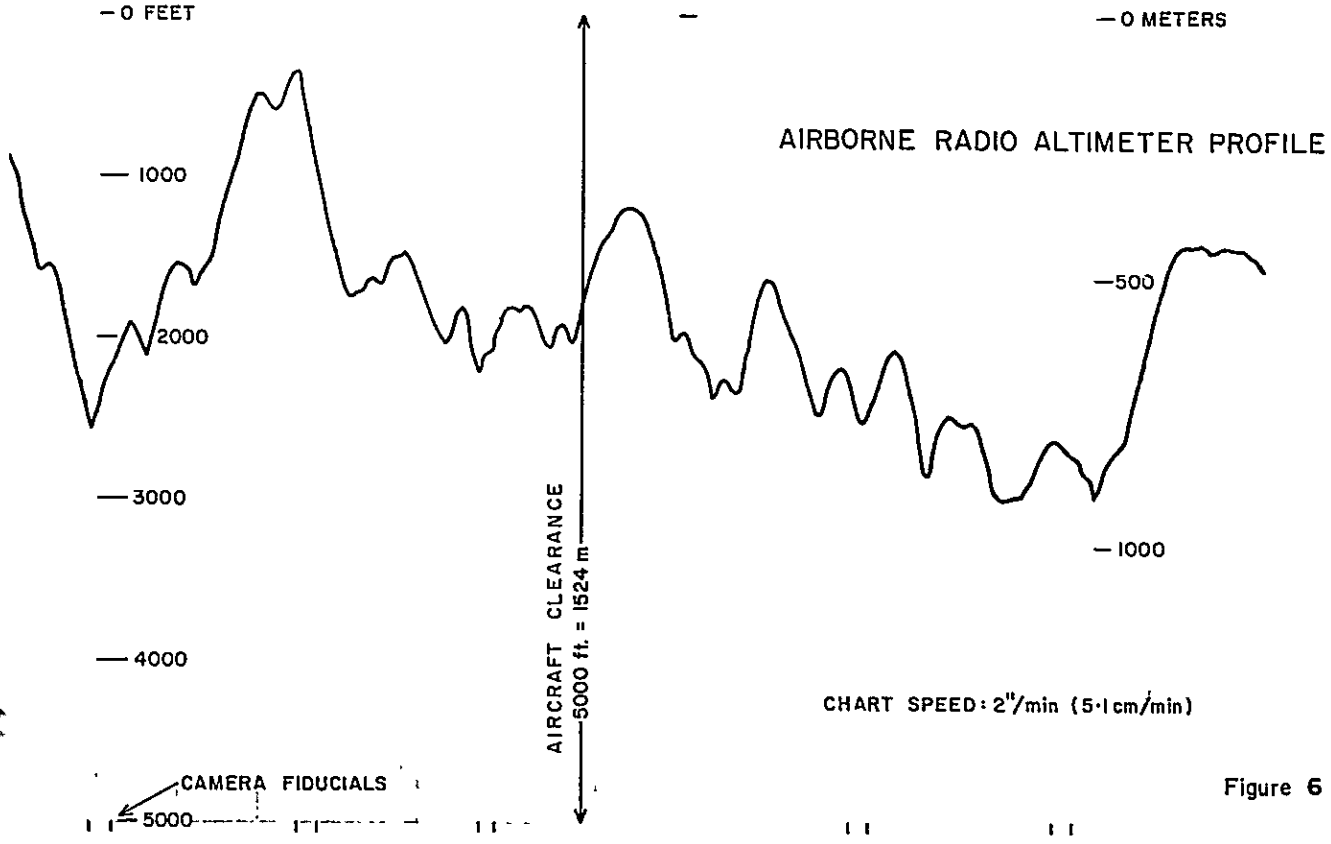

Figure 6

2-3-3 Honeywell Radio Altimeter (HG9050)

This high resolution instrument measures the clearance between aircraft and nearest object. It consists of an electromagnetic pulse-type narrow aperture transmitter operating at 4600 megahertz.

Output from the altimeter system was recorded in analogue form on a rectilinear chart (see Figure 6);

chart speed	: 5 cm./minute
full scale deflection	: 1,524 m. over 12.7 cm. linear
	upper edge = 0 m.

2-3-4 Canadian Applied Research Positioning Camera Mk.VII

This camera uses a 35 mm. film size and was operated in a discrete frame mode. The frame size is 28 mm. lateral, by 25 mm. longitudinal. The focal length is 18.5 mm.. The resulting lateral coverage was approximately 1.5 times the terrain clearance, and the logitudinal coverage somewhat less. Each frame was numbered by a prism system which exposed "veeder" counter numbers on the side of the frame at the moment of exposure. Coincident with every tenth exposure, a fiducial pulse was imprinted on all aerial recording charts. The camera was triggered by the Doppler system, at intervals of 400 m..

2-3-5 Wild RC-9 Super-Wide-Angle Aerial Film Camera

The RC-9 camera has become an important instrument for aerial photography and in the preparation of topographic maps. The principal features of this photogrammetric camera are;

(1) very short focal length objective:
88 mm.

(2) angular field of 120°

(3) image size: 228 mm. x 228 mm.

(4) overlap regulation: by B3B camera intervalometer

The short 88 mm. focal length and 120° angular field permits picture scales at about 60% the altitude necessary using more standard 90° angular field, 152 mm. focal length cameras.

2-4 FIELD SURVEY PERSONNEL

The field survey party mobilized to Palu, Sulawesi, consisted of:

- the Unit Chief (aircraft pilot) and a substitude pilot;
- the Assistant Unit Chief (navigator/aerial photographer);
- a geophysical equipment technician/operator;
- a photographic laboratory technician;
- a geophysical data processing technician;
- an aircraft mechanic.

- the Project Consulting Geophysicist;
- the Project Geophysicist.

2-5 FLIGHT PRODUCTION

The aeromagnetic survey flight pattern included 88 traverses in N-S direction, 9 control lines in E-W direction and a diagonal control line along the coast. The photographic flight pattern included 22 general coverage lines in N-S direction, and 3 control lines in E-W direction, with an additional strip along the Palu River valley.

The chart shown in Figure 7 shows flight production statistics, in line kilometers, for the 30-day period from mobilization to Palu on 28 September to completion of flying on 27 October. Average daily production was:

345.6 line kilometers of magnetics, plus
101.7 line kilometers of photography.

On the basis of first priority to photographic surveying during days of acceptable cloud cover.

A preliminary index of the aerial photography described on a 1/250,000 scale version of the 1/100,000 topographic map (described previously) was submitted to the Indonesian authorities on completion of flying. Figure 8 is a reference index of the photography, with flight lines plotted on the published shaded relief map of the area, enlarged to 1/500,000 scale.

Figure 7

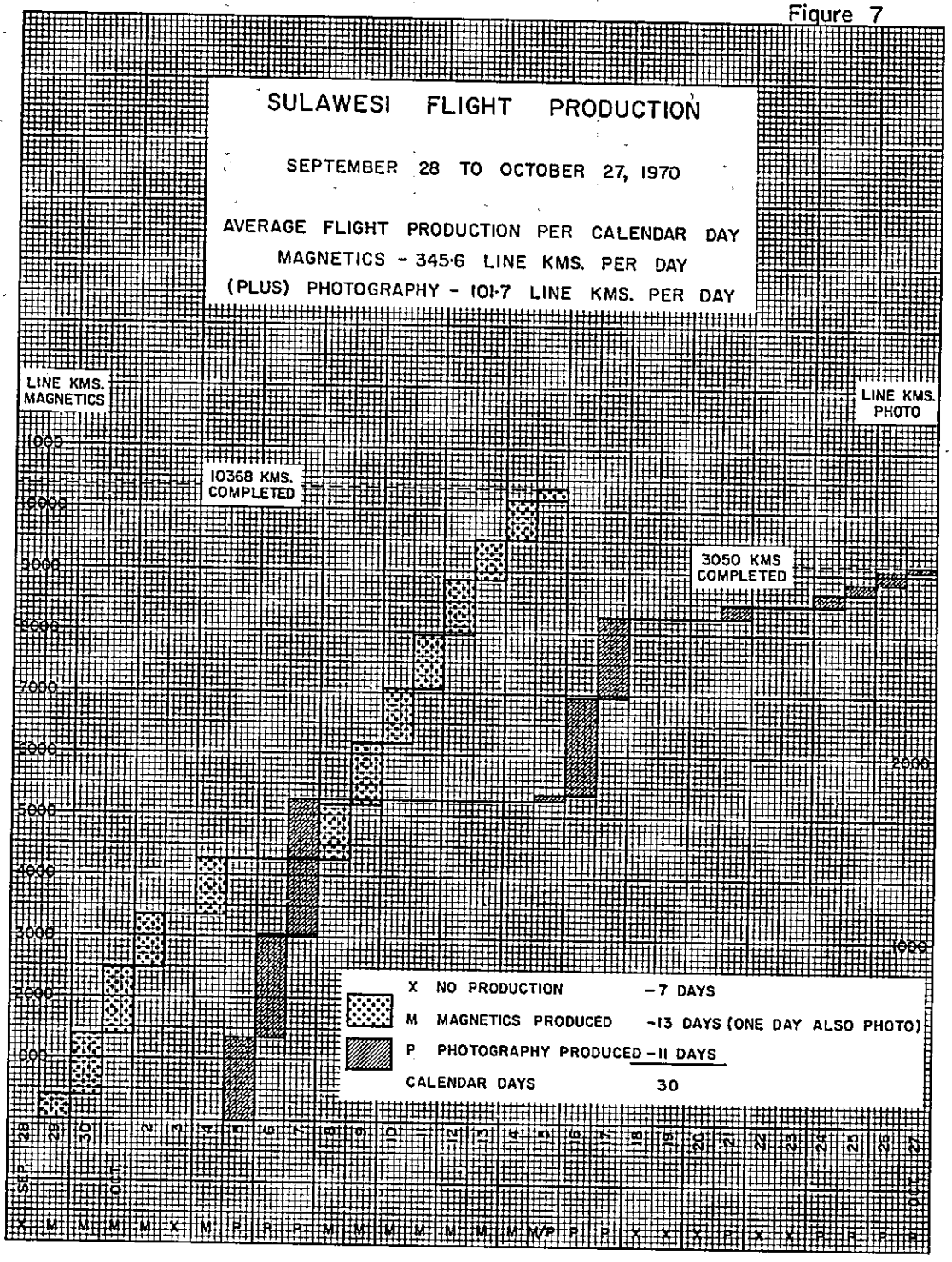

3. GROUND GEOPHYSICAL OPERATIONS

3-1 SURVEY EQUIPMENT PERFORMANCE, PRELIMINARY MAP COMPILATION, MAGNETOMETER SURVEY

In the period October 16 to 23, 1970, Mr. T. Kikuta and Mr. J. W. Prior conducted various geophysical operations at Palu. This work was done in liaison with Mr. J. Komai who represented OTCA. These operations are summarized as follows:

3-1-1 Performance of Aeromagnetic Survey Operation

The performance of aeromagnetic survey operation was evaluated in terms of equipment function and adherence to survey specifications;

- examination of ground monitor magnetometer showed that diurnal variation of the earth's magnetic field during the time of the survey was quite low, in general at a rate of change of less than 20 gammas over an interval of one hour; noise envelope less than 2 gammas;

- inspection of the airborne record showed that the records were virtually clear of nongeological noise greater than one gamma;

- inspection of the radio altimeter record indicated that the altimeter was providing good resolution and adherence to linear calibration over the 0 - 1520 m. range of the recording.

3-1-2 Preliminary Contour Map

The earomagnetic data was compiled in preliminary form at a scale of 1/160,000 and at a contour interval of 50 gammas in order to assess general magnetic character of the survey area and to recommend sites for ground geological and geophysical surveying.

The survey area appeared to be divided into 3 areas of distinguishable magnetic character;

(1) an area of low magnetic relief coinciding fairly well with the Tertiary sedimentary basin adjacent to the Strait of Makassar;

(2) the central part of the survey area was found to be virtually devoid of magnetic expression;

(3) the eastern third of the survey area was found to be characterized by areas of medium to high magnetic relief.

A number of fault zones were interpreted from the controur pattern of the aeromagnetic map; the Palu fault zone (Fossa Sarasina) was well expressed by lineation to the map.

3-1-3 Ground Magnetometer Survey

Because of river flooding and difficulty in road travel, ground magnetometer surveying operations were seriously curtailed. Only one traverse was conducted; along a road leading southeast from

Palu; only a 10 gammas variation was observed over a distance of one km. - corroborating the very low magnetic relief as observed in the airborne survey over this general survey area.

3-2 ROCK MAGNETIZATION MEASUREMENTS

Twelve rock samples were collected by grand geologists during the course of a helicopter-assisted field mapping programme (October - November, 1970). These samples were used for laboratory measurement of rock magnetization - to aid in the subsequent interpretation of the aeromagnetic data. Figure 9 shows the location of each of these samples as well as general geological features.

Table 1 describes the lithology of these samples and the results of the magnetization measurements for susceptibility and remanence. Susceptibility measurements were made using a magnetic susceptibility meter, Bison Instruments Model 3101-A, on loan from the Geological Survey of Japan. Remanent magnetization measurements were made at Tohoku University using a specially designed astatic-type magnetometer.

Eleven of the twelve samples; granite, granodiorite and a metamorphic sample show extremely low magnetization; less than 100×10^{-6} c.g.s. electromagnetic units. This is equivalent to a magnetite content (according to Grant and West 1965 "Interpretation Theory in Applied Geophysics" p.366-8) of less than 0.1%. From this it is apparent that areas within the survey composed of acidic intrusive rocks and sedimentary rocks will have little or no magnetic expression.

The one sample of a basic igneous rock andesite has a magnetization of over 2000 x 10^{-6} c.g.s. units (magnetite content approaching 1%) - far above that for the acidic igneous rocks. Large magnetic relief can therefore be expected for areas underlain by basic igneous rocks.

The above measurements agree with susceptibility-values published by Takesi Nagata (1969);

		$k \times 10^{-6}$ c.g.s.	
Basaltic rocks	:	10,000	
Andesite rocks	:	1,000	*
Granitic rocks	:	100	*
Sediments	:	10	

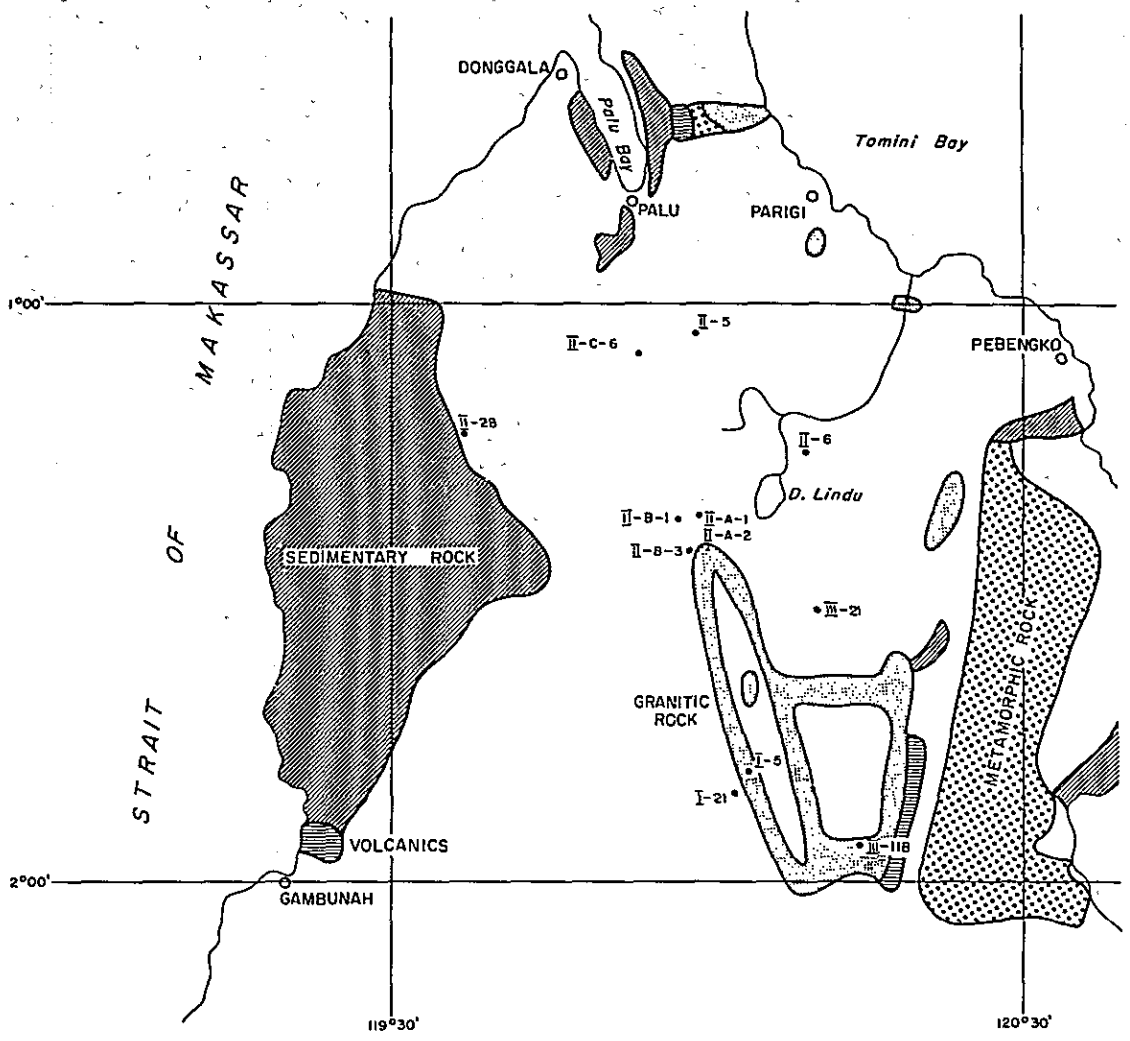

Figure 9

LOCATION MAP*

SHOWING SITES OF ROCK SAMPLES FOR MAGNETIZATION MEASUREMENT

0 25 50 75 100 KM

SCALE 1:1,000,000

*REFERENCE USGS MAP (1965) "GEOLOGIC MAP OF INDONESIA" (1 2,000,000)

Table 1 : ROCK MAGNETIZATION MEASUREMENTS

Sample No.	Magnetic Susceptibility x 10^{-6} c.g.s.e.m.u.	Remanent Magnetization			Lithology
		Intensity x 10^{-6} c.g.s.e.m.u.	Decl.	Incl.	
I-5	<100	2			Biotite granite
I-21	2060 *	170	65.26°E	26.61°N	Hornblende biotite andesite
II-A-1	<100	9	55.32°E	15.08°S	Biotite granodiorite
II-A-2	<100	9	27.30°E	34.52°S	Biotite plagioclase schist
II-B-1	<100	3	102.74°E	32.65°N	Biotite granite
II-B-3	<100	2			Biotite schist
II-C-6	<100	131	11.09°E	58.51°N	Biotite Hornblende granite
II-5	<100	120	3.07°E	61.35°N	Biotite sheared granite
II-6	<100	6	60.21°E	26.42°S	Biotite hornfels
II-30	<100	2	164.05°W	46.32°N	Hornblende dacite
III-11B	100 *	0.4			Biotite granite
III-21	<100	0.5			Quartz sericite chlorite schist

4. AEROMAGNETIC DATA REDUCTION AND COMPILATION

The following is a description of the procedures followed in the reduction and compilation of the aeromagnetic data.

4-1 PRELIMINARY FLIGHT PATH RECOVERY

Using the 35 mm. flight track camera exposures, survey flight path was located by the field data technician in Palu on every third print (228 x 228 mm.) of the high altitude 1/40,000 scale photography. This work was intended as a preliminary to the eventual flight path recovery, using a photomosaic covering the entire survey area.

4-2 PHOTOMOSAIC

An uncontrolled photomosaic was assembled using the high altitude aerial photographs. This photomosaic was produced in nine sheets at a mean scale of 1/50,000. One of the purposes of this mosaic was to provide a means for locating and plotting the aeromagnetic survey flight pattern.

The general purpose of this mosaic was to facilitate compilation of the field geological data and the results of the photogeological interpretation.

For the purposes of this report, the 9 mosaic sheets have been assembled and reduced to provide a 1/250,000 scale composite; Figure 10.

4-3 COMPLETION OF FLIGHT PATH RECOVERY

The photographic mosaics prepared by assembly of the high altitude photographs, at 1/50,000 scale were used for definite plotting of the flight tracks as an initial step in compilation procedure. On this mosaic plot, the location of intersections of magnetic control lines and magnetic traverses was established.

4-4 MAGNETIC BASE MAP CONTROL NETWORK

It had been originally planned to use the 1/50,000 photomosaic as a convenient base to compile the aeromagnetic survey data in the form of a magnetic intensity map. Unfortunately, the Indonesian security officers were unable to quickly clear the high altitude photographs for temporary export to Japan. It was then apparent that insufficient time was available for the execution of a photogrammetric aerotriangulation as a means of establishing a controlled photographic mosaic.

The uncontrolled or "lay-down" mosaic that was prepared and was used for definitive plotting of flight lines and verification of locations of intersections of magnetic control and traverse lines was found to be not sufficiently consistent in terms of uniform horizontal scale for accurate compilation of the magnetic intensity data. An alternative magnetic compilation procedure was therefore adopted.

The technique adopted for compilation may be described as a "multilateration" based on the following data;

(1) recorded Doppler along-track distance measurements;

(2) a number of selected intersections of traverse and control lines which would be accurately located, geographically, on published topographic maps.

4-4-1 Tracking Camera Fiducials and Doppler Navigation

As noted in the technical specifications, exposures of the 35 mm. tracking camera were referenced to the geophysical data recordings by means of a fiducial pen which marks every 10th tracking camera exposure along the margin of the geophysical analogue recording charts. Exposures of the tracking camera were triggured at 0.4 kilometer interval by the along-track distance recording of the aircraft's Doppler navigation system. Although the analogue chart itself was operated at a fixed speed of 7.6 cm./minute; i.e. horizontal scale of the chart varies according to the aircraft speed, the recorded tracking camera fiducials provided a means of accurately determining the horizontal scale of any sector of data recording.

4-4-2 Correspondence of Doppler Measurements and Published Map Distance

A test was done to determine the accuracy of the Doppler along-track distance measurements based on distance measured from the published 1/250,000 scale topographic maps. Five points which are the intersections of survey control lines and traverse lines

situated in the extreme northeast, northwest and southwest limits of the survey area were plotted on the topographic maps;

Table 2: INTERSECTIONS OF SURVEY CONTROL AND TRAVERSE LINES

Point	Control Line	Traverse Line	Latitude	Longitude
1	C-1	T-1	1°00'19" S	120°28'45" E
2	C-1	T-76	1°00'30"	119°29'00"
3	C-3	T-76	1°15'50"	119°27'50"
4	C-3	T-85	1°15'50"	119°20'45"
5	C-9	T-85	1°59'20"	119°20'45"

Points 1 and 2 constitute the east-west base line. Points 2, 3, 4 and 5 constitute two sections of a north-south base line, near the Strait of Makassar coastline. In the case of the length of the east-west base line, along C-1; the Doppler distance was found to coincide with the distance measured from the published topographic map to within 0.06 km..

This was also found to be the case for the northern part of the north-south baseline, i.e. connecting points 2 and 3.

In the case of the segment connecting points 4 and 5, the Doppler measurement exceeded the map distance by only 2%.

These tests demonstrated that satisfactory compilation of the aeromagnetic data could be accomplished using a network of flight line lengths determined from Doppler measurements and the identified track camera intersections between traverse and

control lines.

4-4-3 Control Network, Completion of Magnetic Base Map

A survey control network was established. It consisted of all 9 east-west control lines and every tenth north-south traverse. The length of each line segment was determined from Doppler along-track measurement. The control network was laid out on a geographic base sheet on stable base material at a scale of 1/50,000 on which a reference geographic grid of lines of longitude and latitude at intervals of 10 minutes had been previously drawn (based on Universal Transverse Mercator Grid Tables). Using template materials and equipment usually applied in slotted-template photogrammetry, the control network was mechanically assembled (as illustrated in Figure 11) and attached using the 5 points of Table 2. This established a reference for the network, in terms of its northern and western bounds. All network intersections were then transferred to the geographic base sheet. The Doppler-based control network map was then drawn as a series of interconnecting straight lines in 9 sheets. All remaining traverse lines were located within this network using track camera positioning to identify intersections of traverse and tie lines.

Figure 12 is a 1/250,000 scale reduction composite of the completed survey line network or Magnetic Base Map. This map shows the established pattern of flight lines. Also shown in

FIG. 11 ASSEMBLY OF DOPPLER NETWORK

this map and all maps in which magnetic data and interpretation (Chapter 6) are shown, are 80 "Reference Fiducial" points. These are line intersection points which could be accurately located and plotted on the 1/50,000 scale photo mosaics. They serve as a basis for reference between corresponding magnetic intensity and interpretation map sheets and photomosaic map sheets. The 5 principal points referred to Table 2 correspond with Reference Fiducials 18, 1, 6, 5 and 60 respectively. Table 3 describes the locations of the Reference Fiducials in terms of 35 mm. tracking camera location on both traverse and control lines.

Figure 13 shows, using Figure 12 as a base, the Doppler distance measurements used in constructing the above described survey network Magnetic Base Map.

It should be considered that the distribution of traverse flight lines shown in this map although shown as a series of straight line segments, between control lines, actually involved changes in direction, but it is assumed that these departures from straight lines are minor, and therefore not significant.

Table 3 : REFERENCE FIDUCIAL LOCATIONS

Magnetic Sheet No.	Phto Mosaic Sheet No.	Circuit Fiducial	Line Intersection Position			
			Control Line		Traverse Line	
			No.	35 mm. fid.	No.	35 mm. fid.
1	1	1	C-1	632.2	T-76	2265.6
		2	C-1	590.3	T-64	18.7
		3	C-2	59.5	T-76	2229.3
		4	C-2	103.2	T-64	54.3
		5	C-3	673.3	T-85	4816.5
		6	C-3	706.8	T-76	2195.0
		7	C-3	742.4	T-67	4203.4
2	2	8	C-1	576.2	T-60	635.7
		9	C-1	526.1	T-47	608.0
		10	C-1	474.6	T-33	2375.6
		11	C-2	121.2	T-60	670.2
		12	C-2	180.7	T-44	2272.8
		13	C-2	223.0	T-33	2339.2
		14	C-3	776.8	T-58	2264.2
		15	C-3	835.8	T-42	1235.9
		16	C-3	869.8	T-33	2307.8
3	3	17	C-1	425.8	T-20	1151.5
		18	C-1	354.7	T-1	638.1
		19	C-2	240.9	T-28	53.0
		20	C-2	269.5	T-20	1190.8
		21	C-2	309.0	T-10	681.7
		22	C-2	343.1	T-1	676.0
		23	C-3	888.2	T-28	85.7
		24	C-3	916.6	T-20	1220.4
		25	C-3	958.5	T-10	654.8
		26	C-3	992.6	T-1	704.5
4	4	27	C-4	36.1	T-85	4786.5
		28	C-4	70.0	T-76	2164.7
		29	C-4	114.8	T-65	481.0
		30	C-5	724.2	T-88	4999.1
		31	C-5	679.3	T-76	2126.2
		32	C-5	638.2	T-65	443.2
		33	C-6	788.2	T-88	5029.3
		34	C-6	834.4	T-76	2095.8
		35	C-6	874.7	T-65	412.1
5	5	36	C-4	133.3	T-60	736.7
		37	C-4	172.3	T-49	1330.6
		38	C-4	216.8	T-37	1630.2
		39	C-4	238.5	T-32	1914.3
		40	C-5	617.8	T-60	772.8
		41	C-5	577.5	T-49	1362.7
		42	C-5	533.5	T-37	1598.8
		43	C-5	512.8	T-32	1945.8
		44	C-6	894.5	T-60	805.6
		45	C-6	935.0	T-49	1399.1
		46	C-6	981.3	T-37	1559.7
		47	C-6	1000.0	T-32	1986.8

Table 3 : REFERENCE FIDUCIAL LOCATIONS
(Continued)

Magnetic Sheet No.	Photo Mosaic Sheet No.	Circuit Fiducial	Line Intersection Position			
			Control Line		Traverse Line	
			No.	35 mm. fid.	No.	35 mm. fid.
6	6	48	C-5	499.5	T-28	150.8
		49	C-5	460.9	T-19	2635.1
		50	C-5	396.4	T-2	487.4
		51	C-6	1013.0	T-28	191.2
		52	C-6	1089.7	T-7	2030.0
		53	C-6	1113.7	T-2	444.7
7	7	54	C-7	1473.5	T-85	4676.9
		55	C-7	1439.6	T-76	2056.1
		56	C-7	1406.5	T-67	4063.8
		57	C-8	1563.5	T-83	2667.5
		58	C-8	1590.5	T-76	2021.3
		59	C-8	1625.3	T-67	4029.2
		60	C-9	2223.4	T-85	4613.2
		61	C-9	2191.0	T-76	1991.8
		62	C-9	2155.4	T-67	3999.3
8	8	63	C-7	1378.3	T-60	844.8
		64	C-7	1335.8	T-49	1430.6
		65	C-7	1290.5	T-37	1529.3
		66	C-7	1269.4	T-31	2169.0
		67	C-8	1652.2	T-60	876.8
		68	C-8	1704.0	T-46	352.0
		69	C-8	1757.4	T-32	2054.5
		70	C-9	2126.3	T-59	323.1
		71	C-9	2071.2	T-45	296.4
		72	C-9	2041.7	T-37	1462.4
9	9	73	C-7	1259.0	T-28	220.7
		74	C-7	1234.5	T-22	1040.3
		75	C-7	1160.2	T-2	410.5
		76	C-8	1768.4	T-29	349.7
		77	C-8	1844.3	T-11	970.0
		78	C-8	1872.3	T-1	877.9
		79	C-9	2002.9	T-26	2838.0
		80	C-9	1952.6	T-13	1584.9

4-5 DIURNAL AND GEOMAGNETIC GRADIENT CORRECTION

The distribution of control network intersections at intervals of appriximately 15 km. described in Section 4-3 appeared to be a convenient matrix for diurnal and geo-magnetic field correction. However a number of these locations were found to be in close proximity to high magnetic gradients - an undesirable situation for accurate diurnal correction. Alternative control line/traverse line intersections were then selected in order to retain low magnetic gradient.

The matrix of points selected for adjustment of the magnetic data define a pattern composed of "circuits" connecting "Circuit Fiducials".

4-5-1 Preliminary Datum

For the sake of convenience an arbitrary datum was used in treating the magnetic field intensity analogue profiles. An observed magnetic field intensity of 41,500 gammas was equated to an arbitrary value of 4,500 gammas; viz. an effective datum of 37,000 gammas. It is because of this use of this artificial datum that the resultant Magnetic Intensity Maps (see Section 4-6) show contours such as 4,750 gammas rather than 41,750 gammas the absolute total magnetic intensity or about 650 gammas the residual after removal of the Geomagnetic Reference Field.

4-5-2 Diurnal Correction

Between successive Circuit Fiducials, the monitor magnetometer record was examined to determine magnetic diurnal variation. This variation was found to be quite linear and usually less than 1 or 2 gammas (at most 5 gammas) over the 15 km. line lengths. The diurnal variation was subtracted from the flight magnetic recordings.

4-5-3 Circuit Misclosures

At each Circuit Fiducial, the difference in magnetic field intensity between control and traverse line recordings was determined. This difference (after diurnal correction) is mainly the result of the difference in survey flight elevation between E-W directed lines and N-S directed lines. The circuit misclosure which is the sum of the four differences was then computed; they were found to be quite low, in the order of 4 to 5 gammas, i.e. along a distance of about 60 km.. The circuit misclosure was then distributed linearly along the 4 sides of the circuit.

4-5-4 Geomagnetic Field Correction

A rather steep gradient is evident in the magnetic field intensity profiles - particularly in a N-S direction. This is mainly caused by the Geomagnetic Field Component in the data. This component originates deep within the interior of the earth, near the core-mantle interface approximately 3000 km. below the surface of the earth. The removal of this rather large component would render the data more useful for geological purposes. The Geomagnetic

Component for the survey area was determined on the basis of the International Geomagnetic Reference Field (I.G.R.F.) which has been adopted by the International Association of Geomagnetism and Aeronomy (October 1968). This I.G.R.F. was determined on the basis of high altitude satellite measurements and is expressed in spherical harmonics up to the 8th order and degree.

Input to a computer program (available from the Environmental Science Service Administration, U.S.A.) used to generate the I.G.R.F. at a point in the survey consists of latitude and longitude position, survey elevation and date. Table 4 summarizes the computations that were made at 16 points in the survey area, at intervals of 20' latitude and 25' longitude. For example at 1°40'S, 120°05'E, 1600 m. ASL, for the year 1970, the Geomagnetic Statistics are;

Field Intensity	:	42,231.7 gammas
Field Inclination	:	23.7° above horizontal
Field Declination	:	1.5° E of N

From Table 4 we see that the Geomagnetic Gradient is approximately 5 ɣ/km. N-S and 1 ɣ /km. E-W.

The 16 values of I.G.R.F. intensity were used to construct the Geomagnetic Component, as a contour map covering the survey area. This map was used to establish and plot a 'datum' on each magnetic recording profile. This datum also involves the diurnal correction and distributed circuit misclosure - described previously.

Figure 14 is a composite of the magnetic base map at 1/250,000 scale, annotated to show the progressive adjusted magnetic values at the lattice intersections.

Table 4: GEOMAGNETIC COMPONENT* SULAWESI (1970)

Latitude \ longitude	119°15'E	119°40'E	120°05'E	120°30'E
1°00'S elevation	42044.7 (600 m)	42010.4 (1100 m)	41962.1 (2200 m)	41966.7 (800 m)
1°20'S elevation	42168.5 (600 m)	42132.5 (1200 m)	42101.8 (1500 m)	42064.0 (2100 m)
1°40'S elevation	42299.8 (600 m)	42253.4 (1700 m)	42231.7 (1600 m)	42214.0 (2500 m)
2°00'S elevation	42430.6 (600 m)	42388.9 (1500 m)	42337.4 (2800 m)	42337.1 (1700 m)

*Based on International Geomagnetic Reference Field 1965

4-6 TOTAL MAGNETIC INTENSITY MAP

Locations of 10 gamma magnetic contour intercepts (relative to above datum) and positions of anomaly maximums and minimums were determined and marked on each magnetic profile.

Contour intercepts, maximum and minimum positions, with reference to 35 mm. tracking camera fiducials were then transcribed and located on plotted flight lines in the Magnetic Base Map, scale 1/50,000.

Manual contouring was then used to join the plotted contour intercepts to smoothly represent 10 gamma isoanomaly patterns.

The result after fairdrawing is the Total Magnetic Intensity Map, presente

at three horizontal scales; 1/50,000 (Figure 15, 9 map sheets); 1/100,000 (Figure 16, 3 map sheets) and 1/250,000 (Figure 17, 1 map sheet). Included in these map sheets are survey flight pattern, major geographic details, Reference Fiducials and lines of latitude and longitude. These maps describe variations in the intensity of the earth's magnetic field in the direction of the earth's total field, with respect to the I.G.R.F. approximation of the main earth's field.

4-7 CORRELATION OF MAGNETIC DATA WITH PHOTOMOSAICS

Reference Fiducials described in the Total Magnetic Intensity Maps were also located, with the aid of the 35 mm. tracking camera exposures, on the 1/50,000 scale photomosaics. This was done in order to establish a reference between results plotted using the photomosaic as a base, e.g. data from field geological surveys and photogeological interpretation.

As a general reference, the Circuit Fiducials have also been annotated on a 1/250,000 composite of the 1/50,000 mosaic sheets; Figure 10.

In addition, for purposes of more precise correlation of the magnetic data and the aeromagnetic interpretation results with field data and photogeological interpretation results, intermediate 35 mm. tracking camera fiducials along traverse and control lines have also been plotted on 1/50,000 scale photomosaic work sheets and on working copies of the individual 1/40,000 scale photographs.

5. PROCESSING AND ANALYSIS OF AEROMAGNETIC DATA

5-1 DIGITIZATION

Adequate sampling of aeromagnetic data is accomplished by digitization on a square grid; grid spacing no wider than half the flight line spacing. The 1/50,000 scale aeromagnetic map sheets were assembled and were digitized on a square grid at intervals of 0.635 km. (1/2 inch grid). The grid matrix, 214 by 176, i.e. a total of 37,664 grid points, is oriented north-south. The origin or (1,1) point of this grid is situated at the extreme southwest extremity of line 88 (2°00's, 119°17.1'E). The data was digitized in units of 10 gammas. Verification of the digitization was done using a computer program to identify data associated with abnormally large horizontal gradients.

5-2 REGRESSION PLANE

At the magnetic latitude of the survey area, viz. -25°, anomalies can be expected to consist of adjacent positive and negative peaks - of approximately equal amplitude as shown for the model, at next page.
A tilted plane was fitted to the digitized data using the method of least squares in order to adjust the digitized magnetic data to a zero mean condition. The equation of this planar surface is

$$T_o\ (x,y) = C_1 + C_2x + C_3y$$

where x and y are measured in km., north and east, respectively from the (1,1) point origin of digitization. The computed values of the coefficients are

$$C_1 = 4818.8 \text{ gammas}$$

$$C_2 = -0.4 \text{ gammas/km.}$$

$$C_3 = -0.8 \text{ gammas/km.}$$

At the mid-point of the survey area T_o = 4,742 gammas - comparable to the 4,500 gamma datum adopted in the data reduction (see Section 4-5).

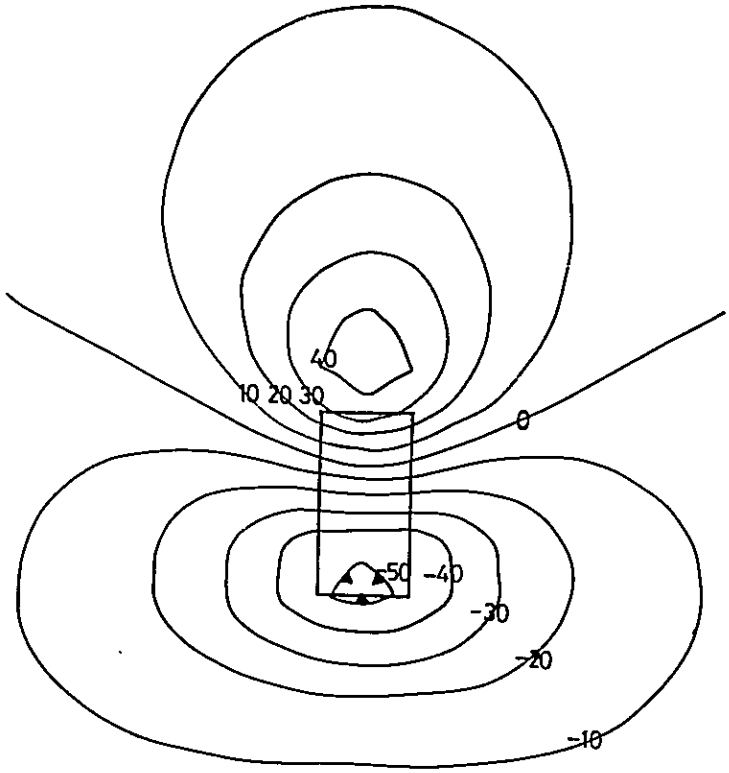

Bottomless prism
Model Anomaly
at $I_E = -25°$

5-3 LOGARITHMIC ENERGY SPECTRUM

The energy spectrum of the digitized aeromagnetic data ΔT was then computed. The method of computation is described by Spector (1968). It consists of first multiplying the data by a "data window"

$$G(x,y) = 1/4 \left(1 + \cos \frac{2\pi x}{L_x}\right) \cdot \left(1 + \cos \frac{2\pi y}{L_y}\right)$$

(where L_x and L_y are the dimensions of the map) in order to obviate the distortion effects that can arise due to the finite size of the digitized map.

The complex spectrum is computed using a numerical version of the equation

$$\Delta\overline{T}(f_x,f_y) = \int_{-\infty}^{\infty}\int_{-\infty}^{\infty} \Delta T(x,y) \cdot G(x,y) \cdot e^{-2\pi i (f_x x + f_y y)} dx\, dy$$

where $f_x = 0, \Delta f_x, 2\Delta f_x, \ldots\ldots\ldots, 1/2\ \Delta x$

$f_y = 0, \Delta f_y, 2\Delta f_y, \ldots\ldots\ldots, 1/2\ \Delta x$

where Δx is the sampling interval 0.635 km.

$1/(2\Delta x)$ is the folding frequency, 0.8 cycles/km. (cpkm)

$\Delta f_x = 1/L_x$, $\Delta f_y = 1/L_y$ (cpkm) are the frequency increments corresponding to the x and y direction of the map.

The complex spectrum can be written in terms of its real and imaginary parts;

$$\Delta\overline{T} = R - iQ$$

The energy spectrum is determined from the relation

$$E(f_x, f_y) = |\Delta\overline{T}|^2 = R^2 + Q^2$$

Only the radial component of the energy spectrum was used for interpretation and is determined by averaging E with respect to azimuth on the frequency plane;

$$E(r)=\frac{1}{2\pi}\int_{o}^{2\pi} Ed\theta$$

where $\theta = \tan^{-1}(f_x/f_y)$

A description of this form of analysis is given by Spector and Grant (1970).

The logarithmic form of the radial component of the energy spectrum is shown in Figure 18. It is apparent that the curve can be divided into three parts; at very low frequencies; 0 to 0.1 cpkm, the rapid drop-off or attenuation of the spectrum with increasing frequency identifies the contribution in the data, from apparently very great depth, viz. 5.5± 0.4 km. below survey altitude. Depth estimates are obtained from the measured slope of the logarithmic spectral curve, using the relation

$$H=\frac{-1}{4\pi}\cdot\frac{\log E_1-\log E_2}{r_1-r_2}$$

At intermediate frequencies the gentler slope of the spectral curve indicates contribution from sources at an average depth of about 1.5 km.. In the remaining part of the spectral curve, i.e. at frequencies greater than 0.25 cpkm. or wavelengths less than 4 km., contributions from magnetized sources within about 200 m. of ground level are indicated.

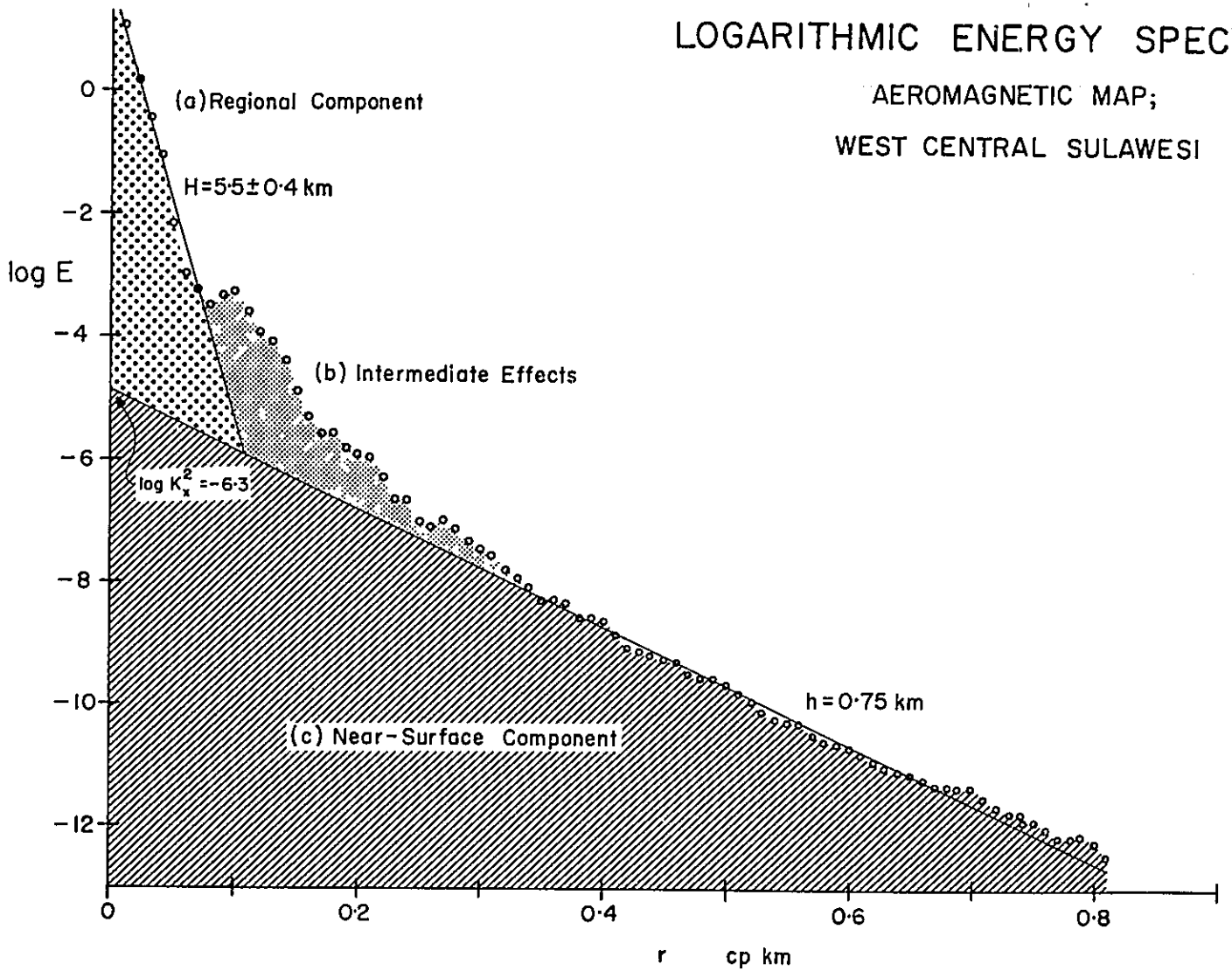
LOGARITHMIC ENERGY SPECTRUMS
AEROMAGNETIC MAP;
WEST CENTRAL SULAWESI
(a) Regional Component
H=5·5±0·4 km
(b) Intermediate Effects
log K_x^2 =-6·3
h=0·75 km
(c) Near-Surface Component
log E
0
-2
-4
-6
-8
-10
-12
0
0·2
0·4
0·6
0·8
r cp km

Figure 18

5-3-1 Significance of Spectral Components

Differences in the slope of the logarithmic energy spectrum in three frequency bands, 0 to 0.1, 0.1 to 0.25 and 0.25 to 0.8 cpkm. were taken to indicate apparent contributions to the data from distributions of magnetization at three distinct depths;

(1) Deep seated sources : average depth 4.9 km. below ground

(2) Intermediate sources : average depth 0.9 km. below ground

(3) Shallow sources : average depth 0.15 km. below ground

There is an alternative and probably more creditable explanation for the shape of the spectrum; that components (1) and (2) are more probably a reflection of the size effect of regional or broad variations in bedrock magnetization, e.g. zones of andesitic volcanics or magnetite-rich gneissic zones separated by far less magnetic granitic units, and that component (3), viz. the shallow sources, is a reflection of individual anomalies within these units, as well as terrain effects resulting from the generally extreme topographic relief of the survey area. This alternative explanation would be verified by coincidence of the areal extent of the regional anomalies (separated out by means of matched filtering, Section 5-4)with distributions of near-surface anomalies.

On the other hand, we do expect to see anomalies of deep origin in the western areas of the survey area, adjacent to the Strait of Makassar, where a rather thick sequence of young (Tertiary) sediments are believed to overly magnetic crystalline rocks.

5-4 MATCHED FILTERING

Matched filtering is a process that is designed to separate near-surface from regional effects at all wavelengths. It is applied effectively if, and only if, near-surface and regional contributions can be separately identified in the energy spectrum of the aeromagnetic map. The matched filter, as its name implies, is designed or constructed directly from measured characteristics of the energy spectrum.

The two depths h and H and the 'power ratio' K_x (see Figure 18) are the necessary parameters for the computation of the filter. To resolve the regional component (i.e. from 'Regional' magnetic basement) filtering is accomplished by convolution of the digitized magnetic data with a weighting function using a numerical version of the following integral;

$$\Delta T_f\ (x,y) = \frac{\int_{-\infty}^{\infty}\int_{-\infty}^{\infty} \Delta T(\xi,\eta)\cdot W(x-\xi,y-\eta)\,d\xi d\eta}{\int_{-\infty}^{\infty}\int_{-\infty}^{\infty} W(\xi,\eta)\,d\xi d\eta}$$

where the weighting function W is computed using the formula

$$W(x,y)=\frac{1}{2\pi}\int_0^{\infty} \frac{rJ_o(pr)}{1+K_x e^{(H-h)r}}\,dr$$

where $p^2 = x^2 + y^2$

A profile of the normalized weighting function is shown in Figure 19a. It is seen that the effective width of the filter is about 7 grid units

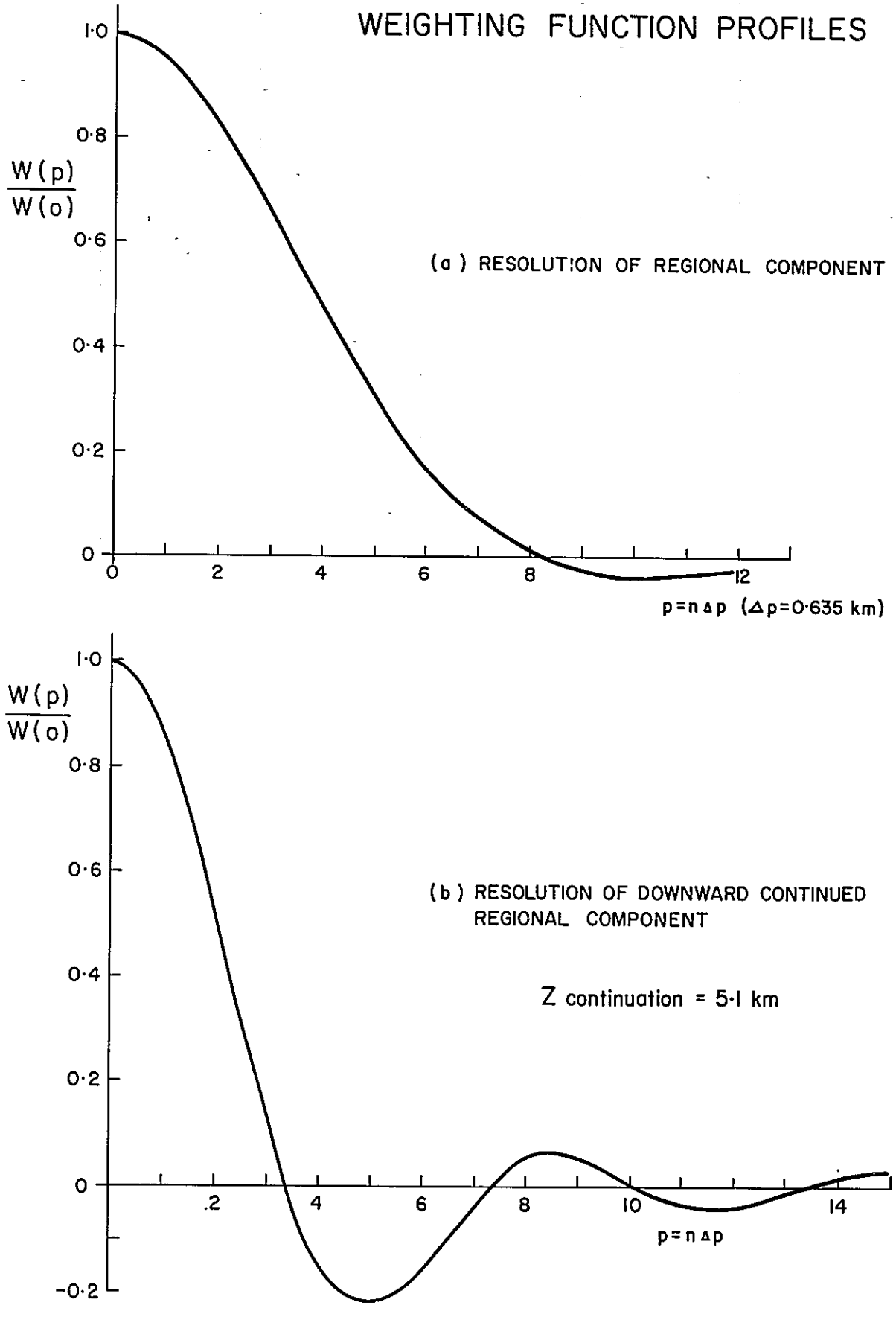
WEIGHTING FUNCTION PROFILES
1·0
0·8
W(p)/W(o)
0·6
0·4
0·2
0
0
2
4
6
8
12
(a) RESOLUTION OF REGIONAL COMPONENT
p=nΔp (Δp=0·635 km)
1·0
W(p)/W(o)
0·8
0·6
0·4
0·2
0
-0·2
.2
4
6
8
10
14
(b) RESOLUTION OF DOWNWARD CONTINUED REGIONAL COMPONENT
Z continuation = 5·1 km
p=nΔp

Figure 19

or 5 km. This is the width of a zone adjacent to the survey map borders that filtering is not entirely effective. A border zone of 5 grid units or 3 km. was left blank in the resulting map.

The Regional Magnetic Component Map is presented at a contour interval of 20 gammas, at two horizontal scales, 1/50,000 (Figure 20, 9 map sheets) and 1/100,000 (Figure 21, 3 map sheets).

5-5 DOWNWARD CONTINUATION AND MAGNETIC POLE REDUCTION OF REGIONAL COMPONENT

As an aid to interpretation, further computer processing was applied to the Regional Magnetic Component data in digital form;

(1) downward continuation of the field in order to increase the resolution of structure;

(2) magnetic pole reduction in order to more clearly see the outline and shape of magnetized units.

5-5-1 Downward Continuation

For the operation of downward continuation, the digitized data is convolved with the following weighting function:

$$W(x,y) = W(p) = \frac{1}{2\pi} \int_0^{\infty} \frac{e^{zr} \cdot J_o(pr)r}{1+K_x e^{(H-h)r}} dr$$

where z is the continuation depth, selected as 5.1 km.. The parameters K_x, H and h are the same as used in the matched

filtering process for determination of the regional component.

A profile of the normalized weighting function W(p)/W(o) is shown in Figure 19b.

A Downward Continued Regional Component Map was produced and contoured at intervals of 20 gammas, at a scale of 1/250,000. This map was used as work material in particular to assist in the identification of fault structures based on the observed truncation, offset or lineation of anomaly patterns.

5-5-2 Magnetic Pole Reduction

Reduction to the magnetic pole of the regional magnetic component map was also undertaken to aid in the structural analysis of the data. Because of the low angle of inclination of the geomagnetic field in the survey area, i.e. about 25° above horizontal, each anomaly is characterized by both a positive and a negative peak which are located near the northern and southern limits of the magnetized source. In addition it is a basic characteristic that at low magnetic field inclinations anomalies due to bodies having east-west orientation will have stronger magnetic expression as compared to anomalies of bodies of north-south orientation. This makes it difficult to identify north-south trending structures as compared to east-west structures. In order to overcome this difficulty and thereby aid the structural interpretation, a second computer processing operation was applied to the regional component data: magnetic pole reduction.

In this process observed anomalies are transformed in such a way as to determine the equivalent anomalies for the case of a vertically inclined magnetic field vector; as shown below;

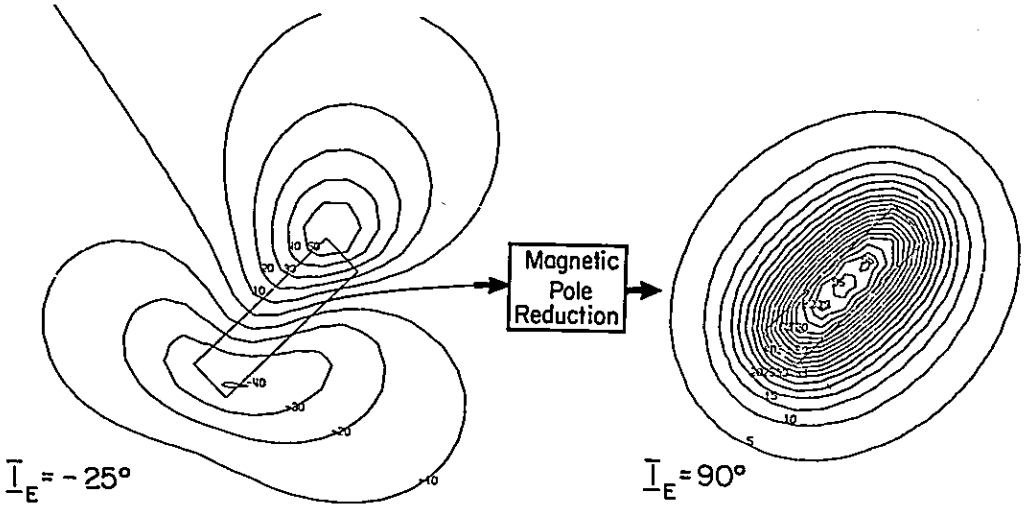

Magnetic pole reduction is done utilizing the computed complex spectrum of the magnetic field intensity map $\Delta\bar{T}$ (see Section 5-3 for a description of the complex spectrum computation). Writing $\Delta\bar{T}$ in terms of its real and imaginary parts,

$$\Delta\bar{T} = R - iQ$$

the magnetic pole reduced complex spectrum is

$$\Delta\bar{T}' = R' - iQ'$$

where $R' = [R (A^2-B^2) - Q (2 AB)] / (A^2 + B^2)^2$

$Q' = [Q (A^2-B^2) + R (2 AB)] / (A^2 + B^2)^2$

and $A = \sin I_E$, $B = \cos I_E \cdot \sin (D_E + \tan^{-1} f_x/f_y)$

where I_E and D_E are respectively the inclination and declination of the earth's field.

The magnetic intensity map reduced to the magnetic pole; $\Delta T'$ is obtained using a numerical version of the inverse Fourier transform;

$$\Delta T' (x,y) = \int_{-\infty}^{\infty}\int_{-\infty}^{\infty} \Delta\overline{T}' (f_x , f_y) \; e^{+2\pi i (f_x x + f_y y)} \, df_x \, df_y$$

The Magnetic Pole Reduced Regional Component Map was produced and contoured at intervals of 20 gammas, at a scale of 1:250,000. This map was used as work material to assist in the interpretation of structure and in the outlining of distinct magnetized zones.

5-6 NEAR-SURFACE MAGNETIC COMPONENT MAP

In order to identify and analyze anomalies which are due to magnetization at relatively shallow depth below ground, the Regional Magnetic Component Data was subtracted from the digitized total intensity data (minus the regression plane, Section 5-2). The residual, or Near-Surface Magnetic Component Map is presented at a contour interval of 10 gammas, at two horizontal scales; 1/50,000 (Figure 22, 9 map sheets)

and 1/100,000 (Figure 23, 3 map sheets).

5-7 MAGNETIC ANOMALY ANALYSIS.

5-7-1 Magnetic Zones

Anomaly patterns represented in the Regional Magnetic Component and Near-Surface Magnetic Component Maps were analyzed to determine;

(a) size and shape of magnetized body source;
(b) depth below ground;
(c) susceptibility contrast;
(d) relationship to topographic effects;
(e) structure.

The analysis to estimate body shape, depth and susceptibility contrast was done following the approach described by Vacquier et al (1951). This approach consists basically of a graphical procedure for matching an observed anomaly with that of a synthetic or artificial anomaly due to a selected model. The basic model selected for this procedure is the "bottomless" prism which has the following assumed characteristics;

(a) vertical sides and a horizontal top;
(b) the bottom of the prism is considered to be at such a great depth that its effect can be assumed insignificant or negligible;

(c) magnetization within the prism is uniform.

5-7-2 Significance of Model

The bottomless prism model is suitable for anomaly analysis in situations where;

(a) contacts of magnetized zones have steep dip, e.g. basic intrusions, gneissic zones;

or (b) the magnetized unit has a thickness much greater than the depth to its top from the magnetometer; e.g. thick volcanic flows.

5-7-3 Anomaly Analysis

The steps followed in executing the anomaly analysis may be described as follows;

(1) A set of synthetic anomaly maps were constructed for a wide variety of model shape, i.e. width and length and orientation, assuming a field inclination of -25°. A large number of these model charts are presented by Vacquier et al (1951). These were supplemented by additional charts obtained using a computer program to generate Calcomp plots of the synthetic maps. The program uses the mathematical expression for the prism as described by Bhattacharyya (1964). Input parameters are intensity, inclination and declination of the earth's field as well as the prism's magnetization vector, prism position, width, length and depth.

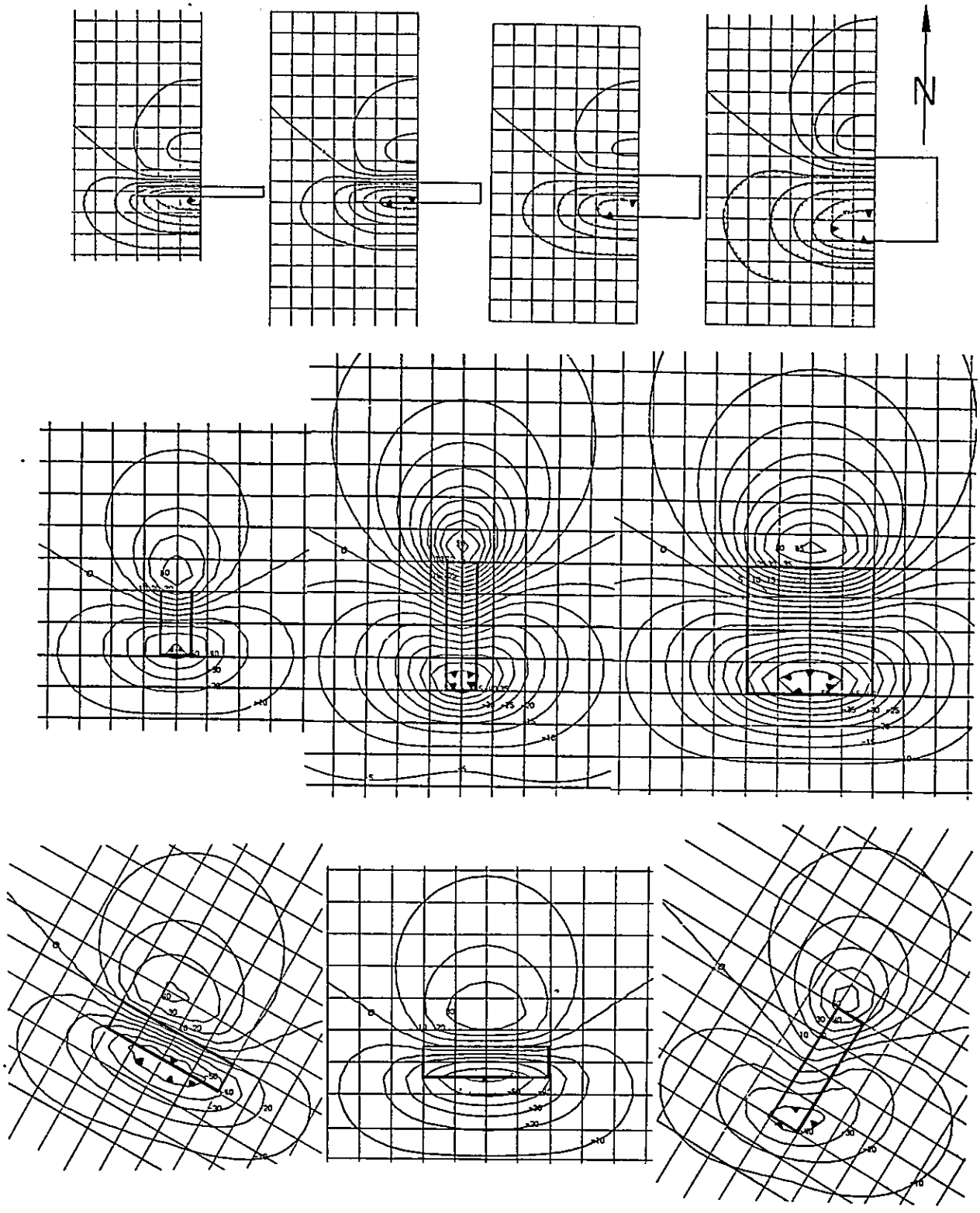

Figure 24

COMPUTED PRISM MODEL ANOMALY CHARTS; $\overline{I}_E = -25°$

Figure 24 shows a number of the model charts compiled for the operation as well as the prism outlines.

(2) For each observed magnetic anomaly, a model anomaly chart was selected which appeared to best approximate the shape characteristics of the observed anomaly. Based on this anomaly match, the model's outline was drawn on the map, to indicate position, length and width of the interpreted "magnetic zone".

(3) Depth determinations (below survey altitude) were made by direct comparison of observed anomaly gradient and model anomaly gradient.

(4) Susceptibility contrasts were determined using the relation

$$K = \frac{1}{T_o} \cdot \frac{\Delta T_{obs}}{\Delta T_{model}} \qquad \left(\text{c.g.s. electromagnetic units}\right)$$

where T_o = 42,100 gammas; the intensity of the earth's field over the general survey area (see Section 4-4), ΔT_{obs} is the amplitude (maximum to minimum) in gammas of the observed anomaly and ΔT_{model} is the model anomaly amplitude.

In some instances, magnetite content as a volume percentage using the empirical relationship given by Takesi Nagata (1969);

volume percent of magnetite : 600 K

(5) Depth determinations were adjusted to elevations in meters below ground using the radar altimeter recording. Because of the rugged topography of the survey area and the associated rapid variations in aircraft-ground clearance, as judged by the radar altimeter records, results of depth determinations were considered significant only to about ±50m..

(6) Topographic association was discerned by inspection of the variations in radar altimeter chart recording. Where it was established that an anomaly coincided with a rapid decrease in aircraft altitude, e.g. in flying over a mountain and that the aircraft altitude was less than 500 meters, a "T"-designation was annotated on the map to signify that the anomaly probably included a substantial topographic effect.

The above forms a description of what was done to analyze the observed anomalies. The analysis was applied to each anomaly that was apparent in the Total Magnetic Intensity Maps and the Regional Magnetic Component Maps.

More rigorous forms of analysis, e.g. use of a wider range of model types, determination of relative proportions of remanence to induced magnetization, etc., were not attempted because

(a) the substantial involvement of topographic effects in

the data

and (b) the reconnaissance nature of the survey, i.e. wide line spacing.

5-8 STRUCTURAL INTERPRETATION AND MAGNETIC UNITS

As indicated in Section 5-7, the position, depth, shape, susceptibility contrast and topographic association of individual "magnetic zones" were determined from anomaly analysis.

5-8-1 Magnetic Units

Areas of the magnetic map that could be distinguished in terms of intensity of magnetization, viz., based on determined susceptibility contrasts, were outlined. These areas are called 'magnetic units' in this report.

The division of the map area according to differences in magnetization was used as an indication of changes in lithology. From rock sample magnetization measurements it has been shown, for example, that granitic rocks can be expected to have a low order of magnetization, i.e. less than 100×10^{-6} c.g.s. units and in contrast basic volcanic rocks have intense magnetization, e.g. in the order of 2000×10^{-6} c.g.s. units.

5-8-2 Identification of Structure

Apparent offset or dislocation of magnetic zones and prolonged lineation of anomaly patterns or magnetic unit contacts were used to identify fault structures.

A discussion of these results, correlated with the results of photogeological interpretation, is presented in Chapter 6.

6. INTERPRETATION

6-1 GEOLOGY OF THE SURVEY AREA: BACKGROUND

Prior to work begun in 1970 under the authority of the OTCA, the geology of a major part of the survey area was largely unknown. An excellent compilation of geological data, secured up to 1948, is presented by Van Bemmelen (1949). In this publication it is seen that only in the extreme northern and southeastern parts of the study area had geological mapping been done and was documented. The following is a descriptive summary of the 6 major structural and lithological features that had been identified;

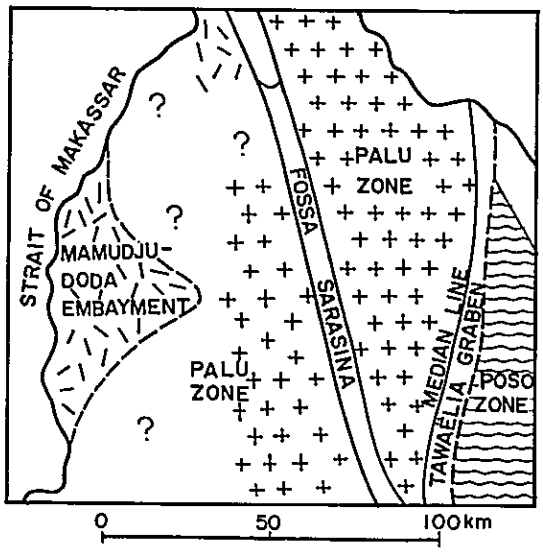

Generalized Geological Map of Sulawesi. Block 4. (Van Bemmelen, 1949)

(a) The Palu Zone occupies the central part of the survey area. It consists mainly of extensive massifs of granodiorite rock that have been intruded from late Mesozoic to Cenozoic time and associated metamorphic rocks; amphibolites - strongly folded sillimanite - biotite gneisses. The zone is bounded to the east by the Median (Fault) Line. It is dissected by the Palu Fault Zone or Graben or Fossa Sarasina. West of the Palu Graben, in the Molengraff Mountains, the Palu Zone consists of granites and associated gneisses and crystalline schists. No active volcanoes are present at this time but igneous activity has been established in the Quaternary by the presence of dacitic tuffs immediately south of the survey area.

Van Bemmelen reports that serpentines, dacites and andesites have been observed in the Palu Zone.

(b) The Poso Zone occupies the eastern margins of the survey area and is separated from the Palu Zone by the Median (Fault) Line. It consists of highly folded metamorphic rocks; principally crystalline schist rich in muscovite. Grade of metamorphism increases from east to the west parts of the Poso Zone. Neither young (e.g. Tertiary) volcanics nor acid plutonic masses have been found in this zone. In contrast, upper Tertiary volcanic activity seems to have been widely distributed west of the Median Line. Rocks of the Poso Zone are apparently much older than those elsewhere in the survey area, ages ranging from Pre-Cambrian to Mesozoic have been suggested.

(c) The Tawaëlia Graben depression is a rather distinct structural sub-zone of the Poso Zone, located east of the Median (Fault) Line and adjacent to the crystalline schists of the Poso Zone to the east, filled with Tertiary sediments and much dacitic and andestic volcanics - which are strongly folded and crushed. The volcanics become the main rock unit in the western and apparently deepest part of the Graben. The fault contact with the Palu Zone granodiorites is marked by mylonitization.

(d) The Mamudju-Doda Tertiary Embayment is a thick basin of strongly folded and faulted Tertiary marine strata; limestone, conglomerates, sandstone, with some coal seams underlying the western coastal belt adjacent to the Strait of Makassar. Sediments with volcanic constituents have been observed. Near the Lariang River a formation of sandy shales and occasional limestones which is at least 5000 m. thick was observed as well as a northerly-trending fault zone.

(e) The Palu Graben or Fossa Sarasina is a young fault valley cutting the Palu Zone obliquely and trending NNW to SSE from Palu Bay to the Median (Fault) Line, a distance of over 200 km.. The valley borders the rugged Molengraff Mountains to the west.

(f) The Median (Fault) Line abruptly cuts off the granodioritic massifs of the Palu Zone and extends over 180 km. from the Gulf of Bone to the Gulf of Gorontalo. Mylonites have been observed along the Median Line. The Median Line appears to be a series of thrust

faults - with movements from west to east.

The succeeding two sections of this chapter deal with;

(a) a detailed description of the Magnetic Units, zones and structures that have been outlined from the magnetics and are correlated with the photogeological interpretation (presented at the time of this report writing as 1/100,000 geological maps);

and (b) a synthesis, summary and conclusions about what has been principally gained by the aeromagnetic survey in terms of a contribution to the geological knowledge of the survey area.

6-2 MAGNETIC UNITS AND STRUCTURE

The results of anomaly analysis, magnetic unit division and structural interpretation are shown on the two sets of interpretation maps;

Near-Surface Magnetic Interpretation Map, Figure 25 (1/50,000 scale)
Figure 26 (1/100,000 scale)

Regional Magnetic Interpretation Map, Figure 27 (1/50,000 scale)
Figure 28 (1/100,000 scale)

The following is a sheet to sheet (according to the 1/50,000 sheet division) description of the Magnetic Units that have been outlined as areas of distinguishable magnetic contrast. This description is referenced to the results of photogeological interpretation. Fault

structures are also described. Where possible, Magnetic Units that have been correlated in both the Regional and Near-Surface Magnetic Component Maps share the same numbering identification.

The following discussion pertains directly to results illustrated in the Near-Surface Magnetic Interpretation Maps and only where cited, to results presented in the Regional Magnetic Interpretation Maps.

6-2-1 Sheet 1

Unit 1; bedrock over much of the survey area is characterized by little or no magnetic expression. Where decreases in aircraft/ground clearance produced magnetic anomalies (of topographic origin), susceptibility contrasts derived from analyses of these anomalies were invariably less than 100×10^{-6} c.g.s. units; i.e. less than 0.1% magnetite content. This was generally the case over granitic rocks.

Areas of unconsolidated sediments, Tertiary sedimentary rocks, slate units, and in particular the felsic or granitic varieties of plutonic rock generally share this magnetic characteristic.

In Sheet 1, Magnetic Unit 1 corresponds with alluvium and Tertiary sedimentary rocks of the Mamudju-Doda Embayment which occupies the western 2/3's of the sheet and granitic rocks in the remainder.

Unit 2; this unit extends east into Sheet 2, and is characterized by NW-trending anomalies with susceptibility contrasts of from 1,000 to 10,000 x 10^{-6} c.g.s. units at depths of from 50 to 600 m. below ground. The unit is expressed by patterns in both the Near-Surface and Regional Magnetic Component Maps and from photogeology is situated in an area which includes both granitic rocks and slate (verified in ground traverses). The magnetic data indicates however that either the granitic rocks and slate have an unusually high magnetite content, i.e. 0.5 to 2% or that a basic intrusive has been introduced.

Unit 3a; in the northcentral part of the sheet, a north-trending zone of low to moderate magnetization; k = 100 to 200 x 10^{-6} units, in an area mapped as Tertiary sediments. Faulting interpreted from the magnetics coincide with photogeological lineaments. This magnetic unit may in part be an indication of volcanics, inter-bedded with the Tertiary sedimentary rocks, or an expression of a very shallow basement, composed of older crystalline rock units underlying the Tertiary sedimentary rocks.

Unit 3b; on line and to the north of Unit 3a, an area of relatively high magnetization, k = 300 - 800 x 10^{-6}

units, corresponding with granitic rocks. This unit suggests the presence of a magnetite-rich gneissic zone. Correspondence is seen in both Regional and Near-Surface Magnetic Component Maps.

Unit 4; a rather lenticular-shaped unit seen in the SE sector of Sheet 1, as an area of low to moderate magnetization, viz. k = 200 to 400 x 10^{-6} c.g.s. (less than 0.2% magnetite). This unit suggests the presence of the same type of lithological unit that is apparent by Unit 3b.

Structure; Two NNE-SSW treding faults are interpreted in the north central part of the Sheet. These faults appear to be offset by an E-W trending faults. There is a good possibility that the NNE-SSW trending faults may actually mark the W-edge of the exposed granites; e.g. the granite/sediments contact might be moved further E from where shown in the photogeological map to near the W-boundaries of Unit 3b. The same may be true with respect to the W limits of Units 3a and 4.

6-2-2 Sheet 2

Unit 1; described in sheet 1, here this unit corresponds with granite and slate units covering most of the

western 2/3's of the sheet.

Unit 2; situated along the west margin of the sheet and is described in Sheet 1.

Unit 7; a N-S trending localized zone situated in the south-central part of the Sheet, adjacent to the Palu Graben, k = 400 - 500 x 10^{-6} units, and is probably a reflection of local magnetite enrichment of granites.

Unit 8 and Unit 8a; an extensive area of low to moderate magnetization; viz., k = 300 -1,000 x 10^{-6} distributed east of the Palu Graben, extending westward from Sheet 3. This unit indicates the presence of an extensive magnetite-rich gneissic/amphibolite zone.

The Unit 8a is a subdivision of Unit 8 and serves to outline areas of higher magnetization; k = 500 -2,000 x 10^{-6} units. The unit is generally situated over granite rocks (and unconsolidated lake deposits of the Palulu Basin). Unit 8a may be a reflection of serpentines in the amphibolite zone.

Little or no magnetic relief is seen over the mapped zone of volcanics, adjacent to the Palu River, south of Bangga.

Structure; A north extension of the Palu Graben is indicated by the magnetic data, particularly in the Regional Component forming the western boundary of a magnetite rich amphibolite/gneiss zone; Magnetic Unit 8.

A number of other northerly trending faults are indicated by the magnetic pattern in the eastern part of the sheet, and correlating with abrupt changes in direction of photo lineaments.

A N-S trending fault is suggested near the west boundary of the sheet, as a contact separating "ultrabasic" Unit 2 from "granitic" Magnetic Unit 1. Some correlation with a series of photogeological lineaments is apparent.

6-2-3 Sheet 3

Unit 1; areas of little or no magnetic expression correlated with granite.

Unit 8 and Sub-Unit 8a; covers much of the west half of the sheet and extending west to Sheet 2 and south to Sheet 6, as a series of areas of moderate to high magnetization; 300 - 1,000 x 10^{-6} c.g.s. units. Anomalies in this unit generally trend north-westerly except where interrupted by faulting.

The distribution of this unit correlates well with those areas mapped as granitic gneiss and/or amphibolite. This Magnetic Unit appears to be a transition from the rather non-magnetic granites which comprise most of the Palu Zone. More magnetic Sub-Unit 8a; $k = 1,000 - 4,000 \times 10^{-6}$ may correspond with zones of increasing basic character, e.g. serpentines. The Regional Component in this sheet shows that Magnetic Unit 8 is developed as an extrusive area of high magnetization and this magnetic relief is probably indicative of the regional change in bedrock lithology.

Unit 12; occupies the eastern margins of the sheet, defined by a distribution of large intensity anomalies that are associated with susceptibility contrasts in the order of $1,000 \times 10^{-6}$ units. The boundary between Magnetic Units 12 and 1 coincides with that indicated in Van Bemmelen's report as the Median Line. Unit 12 thus appears to occupy part of the Tawaëlia Graben and magnetic anomalies probably reflect intrasedimentary volcanics (somewhat lower in magnetite than that to the south). The Graben however does not appear to be well expressed in the photogeology. Unit 12 and the Median Line are poorly expressed in the Regional

Component but are well expressed in maps showing Downward Continuation and also Magnetic Pole Reduction of the Regional Component. The lack of expression in the Regional Component is probably because of the fact that N-S trending features are difficult to identify at equatorial magnetic latitudes.

Structure; As compared to that apparent in Sheets 1 and 2, deformation of rock units in the form of faulting is much more pronounced in this area. The following sets of faults can be identified, according to trend;

(a) NW-SE trending faults, seen in central part of Sheet, extending north from Sheet 6, causing dislocation in the gneiss-amphibolite zones and the Tawaëlia Graben structure;

(b) NE-SW trending faults, seen especially in the SW-sector of the map sheet causing dislocation and termination of identified granite gneiss zones;

(c) an arcuate northly-trending fault in the SE-sector of the map, causing deformation of the Tawaëlia Graben. This may be a thrust fault. Photogeological lineaments follow most of the above fault lines.

As mentioned previously the Mdeian (Fault) Line and

Tawaëlia Graben fault structures can be identified from the magnetics in this sheet.

6-2-4 Sheet 4

Unit 1; similar to that described for Sheet 1; lack of magnetic expression in this case is related to large thickness of Tertiary sediments in the Mamudju-Doda Embayment and to magnetite-poor granitic rocks.

Unit 5; a rather localized area of moderate to high magnetization; k = 200 - 2,200 x 10^{-6} units, seen in the NE sector of the sheet, in an area mainly covered by Tertiary sediments. A distinct change in magnetization is seen in both the Regional and Near-Surface Magnetic Component Maps, signifying a rather discrete change in rock magnetization; probably because of the presence of a gneissic granitic unit underlying about 100 - 300 m. of Tertiary sediments.

Unit 29; in north-central part of sheet, this unit is represented by anomalies in Near-Surface Component Map (k = 400 - 700 x 10^{-6} c.g.s.) and a discrete anomaly in the Regional Component Map (k = 1,200 x 10^{-6} units). The anomalies are seen to originate at a depth of about 500 m. below ground in an area covered by Tertiary sediments and alluvium. The anomalies are probably the expression of either magnetite-rich gneissic granite underlying 500 m.

of sediments or, more probably, Tertiary volcanics within the sedimentary section (see also Unit 30).

Unit 30; located in the central part of sheet, associated with a high magnetization, $1,500 \times 10^{-6}$ units (approximately 0.8% magnetite). Shallow depths are associated, viz. 0 - 100m. much less than that expected for the expected thickness of the sedimentary section. This suggests that these anomalies, and probably those of Unit 29 as well, may be an expression of volcanics within the sedimentary section.

Unit 31 and Sub-Unit 31a; This zone of high intensity anomalies located in the east-central part of Sheet 4 is one of the most conspicuous aeromagnetic features of the survey. Magnetization in the more magnetic Sub-Unit 31a ranges up to $7,500 \times 10^{-6}$ c.g.s. units; i.e. 2-3% magnetite per unit volume. The western fault boundary of this unit closely approximates the photogeological contact between granite and adjacent sedimentary rocks. The very high order of magnetization indicates that the causative source of this prominent magnetic unit is not granite (which is shown in the photogeological interpretation) but an ultrabasic intrusive. Andesitic volcanics

and gabbro seen further south and south-east in Sheets 7, 8 and 9 have similar magnetic response. Ground reconnaissance is certainly recommended in terms of confirming the ultrabasic source indicated by the aeromagnetic data.

Structure; A NNE-SSW trending fault whose west side is down-thrown is interpreted as the boundary of Unit 31. The fault coincides with the photogeological contact between sediments of the Mamudju-Doda Embayment and the granodiorite massif. Based on analysis of Regional Component anomalies a vertical displacement of 500 m. is indicated.

Two NNE-SSW trending faults bounding Units 30 and 29 may also be associated with substantial vertical displacement of the Tertiary sediments.

Two NW-SE trending faults are shown in the NE part of the sheet. These faults are shown extending from Sheet 5. The faults appear to form a graben-like structure bounding the eastern extension of the Mamudju-Doda Embayment.

6-2-5 Sheet 5

Unit 1; areas that are virtually featureless in terms of magnetic expression, corresponding with granite

massifs and to a limited extent slate.

Unit 6; in the extreme northwestern part of sheet, a small localized area of intense anomalies; k = 1,000 to 5,000x 10^{-6} c.g.s. units, similar magnetically to Unit 31a to the southwest (see Sheet 4). Although the area is considered to be granite from photo-geological interpretation, the high magnetization of these rocks indicates the presence of an ultrabasic. Ground reconnaissance is recommended.

Unit 8; in the northeastern sector, a southwest extension from Sheets 3 and 3, areas of low to moderate rock magnetization; in the order of 500 x 10^{-6} c.g.s.. A gneissic/amphibolite zone is apparent, anomaly patterns probably corresponding to fold and foliation patterns.

Unit 14b; see Sheet 6.

Unit 18 and Unit 18a; Unit 18 is well expressed in both Regional and Near-Surface Magnetic Component Maps as an area of greatly increased rock magnetization adjacent to the Palu Graben. Sub-Unit 18a is considered as a possible ultra-basic intrusive.

Unit 20; seen in the south-central part of the sheet, as an area of widely separated anomalies, k = 100 - 400 x 10^{-6} c.g.s. units correlating with gneiss.

Unit 21a; a localized area of high magnetization, i.e. $k = 500$ and $1,300 \times 10^{-6}$ extending from Unit 21 in Sheet 8. Although coincident with gneisses the high rock magnetization in this magnetic unit suggests the presence of andesitic volcanics.

A number of rather isolated volcanic units are indicated in the photogeological interpretation along the Palu River. None of these appears to have significant magnetic expression.

Structure; The Palu River Graben can be mapped by apparent offset and truncation of magnetic anomalies in both Near-Surface and Regional Magnetic Component Maps.

Two long continuous NW-SE trending faults are interpreted as crossing the western part of the sheet. Some photogeological correlation is seen in the form of lineaments, particularly for the southern of the two magnetic faults.

6-2-6 Sheet 6

Unit 1; gross areas of little or no magnetic expression, viz. susceptibllity contrasts of 100×10^{-6} and less, covering central part of sheet and which correspond with granodioritic massifs in the western part of the sheet and crystalline schists

of the Poso Zone in the eastern parts of the sheet.

Unit 8 and Unit 8a; see Sheet 3.

Unit 12; in the northeast sector of sheet a rather narrow zone of east-trending anomalies associated with moderate to high rock magnetization; 300 - 800 x 10^{-6} c.g.s. units. Based on the photogeology this unit is located entirely within a gneissic unit, however there is a strong suggestion that this unit is due to andesitic volcanics of the Tawaëlia Graben, i.e. a northern extension of Unit 17.

Unit 14a and Unit 14b; narrow zones of elongate anomalies of moderate intensity in northwest and west-central parts of sheet; susceptibility contrasts in the range 100 - 500 x 10^{-6} c.g.s. units. These anomalies are probably a reflection of granite gneiss zoning.

Unit 15; in the southwestern sector of the map reflecting a rather distinct and localized change in rock magnetication; rather intense anomalies associated with susceptibility contrasts in the range 400 to 4,000 x 10^{-6} c.g.s.. Unit 15 is located in an area mapped as granitic, however the intense magnetization indicated for these rocks is more indicative of andesitic volcanics (examples seen most clearly in

Sheet 8). Ground investigation is certainly recommended to confirm that this rock unit is an extension of the andesite volcanics in the southern part of Sheet 8 or an ultrabasic intrusive.

Unit 17; in the eastern part of the sheet two long narrow chains of large amplitude anomalies associated with magnetication in the order of 1,500 to 2,500 x 10^{-6} c.g.s. units; i.e. a magnetite content of about 0.8%. Unit 17 is situated in an area covered by lake deposits of the Paanto Basin, adjacent to the crystalline schist of the Poso Zone area. A probable source of these anomalies may be a down-faulted sequence of recent andesitic volcanics; the Tawaëlia Graben.

Unit 17a; lies immediately adjacent to Unit 17 and appears to be a less magnetized sub-unit of Unit 17. Because the area is covered by recent sediments, the unit's lithologica. identification is unknown in terms of photogeological interpretation. Based on magnetic expression a likely source of this unit may be Tertiary volcanics, within the sedimentary section of the Tawaëlia Graben.

Unit 19; a localized area of rather moderate amplitude an anomalies; susceptibility contrasts in the range

$200 - 500 \times 10^{-6}$ c.g.s.. This unit sppears to be a southern extension of Units 17 and 17a and probably shares a similar origin; recent volcanics in the Tawaëlia Graben adjacent to the crystalline schist complex to the east - although photogeological interpretation has indicated that the magnetic unit coincides with granite.

Structure; Principal structural features evident in this map sheet are (1) a series of long NW-SE and NE-SW trending faults that appear to extend continuously across the breadth of the sheet; i.e. through the granitic massif dominating the central part of the sheet. Some of these faults coincide with photo-geological lineaments and (2) the Tawäelia Graben structure adjacent to the Poso Zone crystalline schist complex.

6-2-7 Sheet 7

Unit 1; areas of virtually no magnetic expression corresponding with those photogeological units indicated as sediments and alluvium.

Unit 32; a rather local increase in rock magnetization; $k = 200 - 400 \times 10^{-6}$ c.g.s. seen to the northeast. Similarity in magnetization suggests that this unit

shares a common identity to that ascribed for Units 29, 30 and 31 to the north. A volcanic member within the sedimentary section, here at a depth of 350 m. below ground.

Unit 33; is located in the southwest sector of the map as an area of low to moderate rock magnetization; k = 200 - 600 x 10^{-6} c.g.s.. It is on the basis of lower magnetization that this is mapped as distinct from Unit 34 located immediately to the east. Anomaly sources in this unit lie at depths of -150 to -400 m. below ground, covered by Tertiary sediments. Unit 33 is similar to Units 32, 31, 30, 29; i.e. moderate to low magnetization in an area covered by sediments and may therefore be due to volcanics in the sedimentary section.

Unit 33a; is located immediately SW of Unit 33 and is similar to it in terms of intensity of magnetization; 300 - 500 x 10^{-6} c.g.s.. This unit or at least its northern part, coincides with an area mapped as Kentallenite in older geological maps of Sulawesi. Kentallenite is an acidic intrusive rock type similar to Monzonite. The low order of magnetization does not prevent the interpretation of the unit as due to Kentallenite, but neither does it exclude the possibility of

extrusive volcanics within the sedimentary section.

Unit 34 and Sub-Unit 34a; are located in the south-central part of the sheet, as an area of relatively moderate to high rock magnetization; 100 - 1,000 x 10^{-6} c.g.s.. Good coincidence between this unit and andesitic volcanics outlined in the photogeological interpretation is apparent. Sub-Unit 34a indicates those areas of higher than normal magnetization; viz. 2,000 x 10^{-6} c.g.s. within Unit 34. Dykes mapped in the photogeological interpretation do not appear to have distinctive magnetization as compared to the surrounding andesitic extrusives.

An area partially enclosed by Unit 34, is identified as Unit 1 because of magnetization in the order of 100 x 10^{-6} c.g.s. or less. This should be taken to indicate a possible change in volcanic facies, e.g. a transition to a more felsic extrusive rock.

Outlined in the Regional Component Interpretation Map is a much more extensive but well defined area of high rock magnetization (k = 2,000 - 2,200 x 10^{-6} c.g.s.) corresponding with Unit 34, probably due to the basic intrusive at depth from which the andesites originated. This intrusive also appears to be linked geographically to Units 33 and 33a, considered to be volcanics

within the Tertiary section.

Structure ; The andesitic volcanics of Unit 34 are seen to be deformed and dislocated by a series of NE-trending faults. The most westerly of these, coinciding with photogeological lineament 20 is considered to be a normal fault, west side downthrown a minimum of 200 m.

The WNW-trending faults in the NE map sector concide with photogeological lineaments affecting Tertiary sediments - this helps to corroborate the interpretation of adjacent magnetic units as due to volcanics within the sedimentary section.

6-2-8 Sheet 8

Unit 1; areas of minor magnetic expression underlain by granite and slate.

Unit 21; to the northeast, a series of areas of low rock magnetization ($k = 200 - 300 \times 10^{-6}$ c.g.s.) corresponding to granite gneiss.

Unit 23; similar to Unit 21 in terms of moderate magnetic expression, located within slates - but appearing to connect two ultrabasic gabbro intrusives, Units 24a and 24b.

Unit 24a and
Unit 24b; outline two localized areas characterized by very intense magnetic expression. The cause of these anomalies appears to be ultrabasic intrusives (gabbro). The deep-seated origin of the intrusive is well expressed in the Regional Magnetic Component Map.

Unit 26; in the west-central part of sheet, a very localized area of higher than background magnetization; $k = 700 - 900 \times 10^{-6}$ c.g.s. units, in area mapped as granite. These anomalies may be due to a more basic form of intrusive associated with granite, e.g. gabbro, similar to that evident by Units 24a, 24b and 27.

Unit 27; two very small areas in the central part of the sheet, similar to Units 24a, 24b and 26, probably sharing the same lithological identity. The western area is located at the contact between granite and slate. This contact position may be significant in terms of economic mineralization.

Unit 28 and
Sub-Unit 28a; this unit located in the south-eastern sector and its outline coincides quite closely to that mapped as andesitic volcanics. Rock magnetization is relatively high, viz. $200 - 800 \times 10^{-6}$ c.g.s. in the

more magnetic Sub-Unit 28a. The andesitic zone is well expressed in both the Near-Surface and Regional Component Maps.

Unit 29; see Sheet 9.

Structure; Two NW-SE trending faults are seen to border or truncate the magnetic andesitic unit in the southeast part of the map. One of these faults borders an interpreted gabbro intrusive. A portion of the Palu Graben structure is seen along the northeastern margins of the sheet.

6-2-9 Sheet 9

Unit 1; areas in which rock magnetization is generally quite low, i.e. susceptibilities in the range 50 - 200 x 10^{-6} c.g.s., corresponding with Palu Zone granite and much of the crystalline schist complex of the Poso Zone.

Unit 13; areas of low to moderate magnetization; k = 200 - 400 x 10^{-6} c.g.s. within the crystalline schist complex.

Unit 19; this unit extends southerly across the sheet, from Sheet 6. Rock magnetization is high; 400 - 1,000 x 10^{-6} c.g.s.. The location of the unit generally coincides with that mapped as Tertiary sediments

which include highly magnetic volcanic materials. The magnetic data verifies that this sedimentary unit includes a volcanic unit and that this unit is quite continuously distributed in what is termed in the photogeological interpretation; the "Tawäelia Graben".

Unit 19a; unit describes areas within Unit 19 that have excessively high magnetization; 2,000 - 5,000 x 10^{-6} c.g.s. units, i.e. a magnetite content in excess of 1%. According to the photogeological interpretation Unit 19a, south of control line 8, southeast of the villages of Bomba and Pada, coincides with dolerite; a basic intrusive rock type. These may have been the areas from which the volcanic material deposited in the Tawäelia Graben may have originated, viz., ultrabasic intrusives.

Unit 22; in the northwest part of the sheet, an area of intense magnetization; k = 2,700 x 10^{-6} c.g.s. that is well expressed in both Near-Surface and Regional Component Maps, located in the southern end of a granitic gneiss zone. The unit is bounded by a ENE - WSW trending fault. The high magnetization however suggests that a basic intrusive is present. Confirmation by ground reconnaissance is recommended. In

addition attention. should be given to the possibility of mineralization near the fault zone forming the northern boundary of this unit.

Unit 28 and Unit 28a; this area of high magnetization (k = 1,100 - 2,600 x 10^{-6} c.g.s.) is an eastern extension of that seen in Sheet 8 corresponding with andesitic volcanics. The magnetics therefore suggest an eastward extension of the andesitic volcancis, from that shown in the photogeological mapping.

Unit 29; seen along the western margin of the sheet, moderate to high magnetization; 300 - 1,100 x 10^{-6} c.g.s.. In view of similarity with Unit 28 this unit is probably a northern outlier of andesitic volcanics.

Structure; The most distinct structure in this map sheet is the so-called Tawaëlia Graben adjacent to the crystalline schist complex to the east, trending north-south and containing volcanic members within a sedimentary section. The Graben appears to be dislocated in places by a series of westerly trending faults.

The Palu Graben is expressed in both the Regional and Near-Surface Magnetic Component Maps.

6-3 SYNTHESIS

Based on a detailed analysis of the aeromagnetic data, with reference to the results of a photogeological interpretation, the following general remarks can be said concerning the geology of the survey area (as described in Figure 29);

6-3-1 Major Structural Units

The general structural unit division of the area, described by Van Bemmelen (1949) agrees with the gross structural pattern evident from the aeromagnetic data;

(1) The Palu Zone: consists of, in the main, extensive granodioritic massifs characterized by little or no magnetic response because of rock magnetization rarely in excess of 100×10^{-6} c.g.s. units; magnetite content of less than 0.1 per-cent.

The granodioritic massifs appear on the basis of magnetic property to be quite uniform in composition over large distances.

(2) The Palu Graben or Fossa Sarasina can be mapped as a virtually continuous structure between the north and the south limits of the survey area. The eastern fault of the structure is relatively more apparent in the magnetics and has been called the Palu Fault.

(3) The Median Line separating Palu Zone granitic rocks from weakly magnetic Poso Zone metamorphic units can be distinguished as the western edge of a graben sub-structure of the Poso Zone; the Tawaëlia Graben, containing highly magnetic volcanics. The Median Line has suffered dislocation by a series of E-W and NW-SE trending faults.

(4) The Mamudju-Doda Embayment filled with virtually non-magnetic Tertiary sediments also contains in places magnetic volcanics within the sedimentary section.

6-3-2 Ultra Basic Intrusives

A number of zones of high rock magnetization are prominent in the aeromagnetic data, both in the Near-Surface and in particular, in the Regional Mangetic Component Maps. They have been interpreted as probable sites of ultrabasic intrusion. Nine of these sites are situated in the Palu Zone; 3 of which are correlated with either andesitic volcanics or intrusive gabbro, and 2 are located within the Tawaëlia Graben volcanics.

Figure 29

GENERALIZED GEOLOGICAL SYNTHESIS

SCALE 1:500,000

0 20 40 Km.

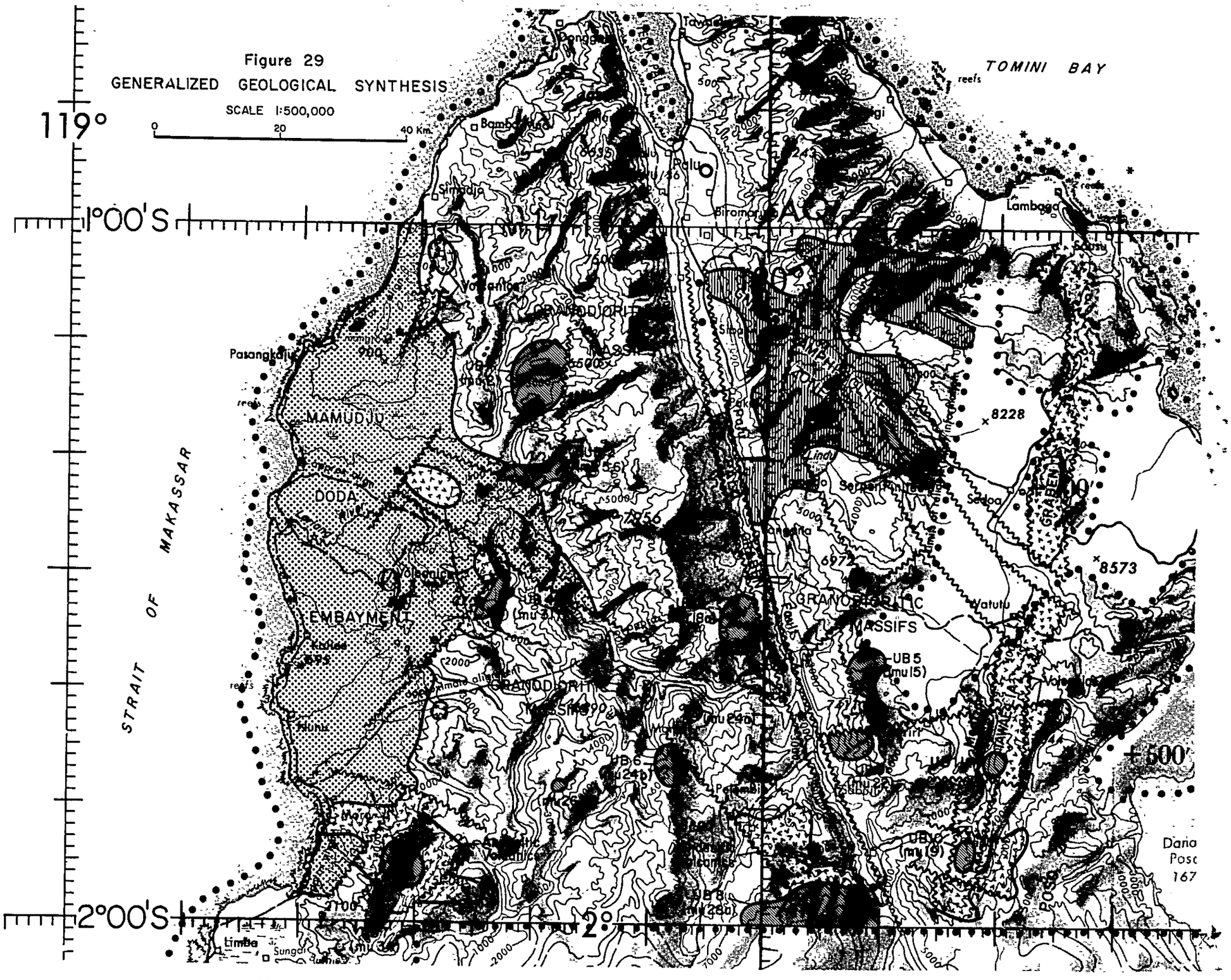

Table 5 is a list of these interpreted ultrabasic zones and their positions (see Figure 29);

Table 5: LOCATION OF INTERPRETED ULTRABASIC ZONES

	Magnetic Unit	Location		Photogeological Association
UB_1	2	1°12'S	119°40'E	granite, slate
UB_2	5,6	1°21'	119°40'	granite, slate
UB_3	18a	1°33'	119°57'	granite, adjacent to palu Graben
UB_4	31	1°31'	119°35'	granite
UB_5	15	1°38'	120°09'	granite
UB_6	24b,24a	1°46'	119°53'	granite, gabbro
UB_7	34a	1°55'	119°28'	andesitic volcanics
UB_8	28a	1°57'	120°05'	andesitic volcanics
UB_9	22	1°45'	120°07'	gneiss
UB_{10}	19a	1°54'	120°17'	Tawaëlia Graben
UB_{11}	19a	1°46'	120°20'	Tawaëlia Graben

The above outlined ultra basic zones may have been the cores or plugs of ancient (Tertiary) volcanoes that emerged as the more basic magmatic phases of the granitic batholiths. In addition because observed presence of magnetic volcanics within the Tertiary sediments of the Mamudju-Doda Embayment and the Tawaëlia Graben,it is likely that igneous activity occurred during the development stages of these two structures and possibly also the Palu Graben.

6-3-3 Gneiss/Amphibolite Metamorphic Rock Zone

Zones of moderate to large amplitude anomalies trending generally NW-SE are prevalent over a wide area in Sheets 2 and 3. The zones

are grouped as Magnetic Unit 8 and they correlate with gneissic zones in the photogeological maps. The aeromagnetic data, however, indicates that this area of regional metamorphism is much more extensively distributed than indicated in the photogeology. A NW-SE trending zone of especially high magnitude anomalies in Sheet 3 (Unit 8a) suggest the presence of serpentinites.

6-3-4 Development of Mamudju-Doda Embayment

A number of faults are interpreted along the margins of the Mamudju-Doda Embayment. These faults are probably normal faults with large vertical displacement. The eastern extension of the Embayment in the vicinity of the Lariang River is probably a graben-like depression. Some of the faulting appears to have occurred subsequent to the distribution of volcanics.

As discussed previously, part of the development of the Mamudju-Doda Embayment, the development of the Palu Graben and the Tawaëlia Graben may have coincided in time, subsequent to the last extrusion of andesitic volcanics.

6-4 RECOMMENDATIONS: FUTURE GEOPHYSICAL SURVEYING

The aeromagnetic survey has succeeded in presenting data that contributes to the understanding of the study area's geology, particularly in terms of those areas that were virtually unknown in terms of published geological mapping. Future exploration phases will be directed towards the search for base metals mineralization, in the form of more detailed geophysical surveys and geological mapping of the contacts and interior of individual lithological and structural units, e.g.

- the ultrabasic intrusions
- the metamorphic zones, with special attention given to possible serpentinization
- faults and shear zones adjacent to and dislocating the Median (Fault) Line and adjacent Tawaëlia Graben.

Geophysical surveying for purposes of locating conductive sulphide mineralization would be most efficiently done using airborne platforms, e.g. helicopter and/or STOL aircraft. Recommended survey systems are:

1. Helicopter mounted rigid boom EM system consisting of coaxial vertical transmitter and receiver coils 10 m. apart in a rigid boom 30 m. below helicopter.

   The effective penetration depth of this system is a function of ground electrical conductivity, but is generally about 60 to 80 m. below the receiver/transmitter configuration. Taking general tree height, the great depth of surface rock weathering, the severe EM response due to variations in aircraft/ground clearance, however may limit the effectiveness of this system.

2. Helicopter or Fixed Wing VLF-EM Surveying is a rather new type of approach which utilizes the EM field generated by military radio transmitters in the range 15,000 to 25,000 Hertz, located in Australia, Hawaii and Japan. VLF-EM surveying is least affected by topographic relief and tree cover because of the much lower rate of signal attenuation with height as compared to the rigid boom devices. The high operating frequencies employed allow for high response from

mineralized bodies of relatively small dimensions, e.g. "disconnected" sulphide mineralization, sheared contacts, breccia zones, faults and alteration zones.

Magnetometer surveying is recommended in conjunction with EM surveying.

Radiometric and ground gravity surveying are not recommended because of the very high topographic relief of the area and in the use of gravity surveying the lack of accurate large scale topographic maps for purposes of making terrain correction.

The interpretation of the survey data embodied in this report is essentially a geophysical appraisal of the area; as such it can incorporate only as much geological and geophysical information as the interpreter has available at the time. It should be judiciously used, therefore, as a guide only by geologists thoroughly familiar with the area and who are in a better position as time passes to evaluate the geological significance of any particular feature. With additional information such as that provided by ground and detailed airborne surveys, it may be possible to down- or up-grade features discussed or identified in this report that take on less or greater significance than was first apparent to the interpreter.

Appendix

REFERENCES

Bhattacharyya, B. K. 1964 "Magnetic Anomalies Due to Prism-Shaped Bodies with Arbitrary Polalization" GEOPHYSICS, V.21, pp.517-531

Grant, F. S., West, G. F. 1965 "Interpretation Theory in Applied Geophysics" McGraw Hill, New York, pp. 366-368

Malahoff, A. 1969 "Magnetic Studies over Volcanics in the Earth's Crust and Upper Mantle", pp.436-446 A.G.U. Geophysical Monograph 13

Nagata, T. 1969 "Reduction of Geomagnetic Data and Interpretation of Anomalies in the Earth's Crust and Upper Mantle", pp.391-398 A.G.U. Geophysical Monograph 13

Spector, A. 1968 "Spectral Analysis of Aero-Magnetic Maps" Ph. D. Thesis, University of Toronto

Spector, A., Grant, F. S. 1970 "Statistical Models for Interpreting Aeromagnetic Data" GEOPHYSICS, V.35, pp.293-302

United States Geological Survey 1965 "Geological Map of Indonesia" Map 1-414, Scale 1:2,000,000

U. S. S. R. Academy of Sciences 1966 "Tectonic Map of Asia" Scale 1:5,000,000

Vacquier, V., Steenland, N. C., Henderson, R. G. and Zietz, I. 1955 "Interpretation of Aeromagnetic Maps" Geol. Soc. America Memoir 47

Van Bemmelen, R. W. 1949 "The Geology of Indonesia" Govt. Printing Office, The Hague.